*Article*

# Effect of Process Conditions on Hydro-Char Characteristics and Chemical Composition of Aqueous and Gaseous Products by Hydrothermal Processing of Corn Stover with Hot Compressed $H_2O$: Structural Evolution of Hydro-Char and Kinetics of Corn Stover Decomposition

**Tiago Teribele[1], Maria Elizabeth Gemaque Costa[1], Conceição de Maria Sales da Silva[1], Lia Martins Pereira[1], Lucas Pinto Bernar[1], Douglas Alberto Rocha de Castro[1], Fernanda Paula da Costa Assunção[2], Marcelo Costa Santos[3], Isaque Wilkson de Sousa Brandão[4], Clícia Joana Neves Fonseca[5], Maja Shultze[6], Thomas Hofmann[6], Sammy Jonatan Bremer[7] and Nélio Machado[1,2,4]***

[1] Graduate Program of Natural Resources Engineering of Amazon, Rua Corrêa N° 1, Campus Profissional-UFPA, Belém 66075-110, Brazil; t.teribele@outlook.com (T.T); gemaquebeth@ufpa.br (M.E.G.C.); concisales@ufpa.br (C.d.M.S.d.S.); liapereira@ufpa.br (L.M.P.); lucas.bernar7@gmail.com (L.P.B.); douglas-castro87@hotmail.com (D.A.R.d.C.)
[2] Graduate Program of Civil Engineering, Rua Corrêa N° 1, Campus Profissional-UFPA, Belém 66075-110, Brazil; fernanda.assuncao@itec.ufpa.br (F.P.d.C.A.)
[3] Graduate Program of Chemical Engineering, Rua Corrêa N° 1, Campus Profissional-UFPA, Belém 66075-110, Brazil; marcelo.santos@ufra.edu.br (M.C.S.)
[4] Faculty of Sanitary and Environmental Engineering, Rua Corrêa N° 1, Campus Profissional-UFPA, Belém 66075-900, Brazil; isaquebrand@gmail.com (I.W.d.S.B)
[5] Graduate Program of Materials Science-IME, Praça General Tibúrcio N°. 80, Rio de Janeiro 22290-270, Brazil; clicia.fonseca@ime.eb.br (C.J.N.F.)
[6] Leibnitz-Institüt für Agrartechnik Potsdam-Bornin e.V, Department of Postharvest Technology, Max-Eyth-Alee 100, Potsdam 14469, Germany; mschultze@atb-potsdam.de (M.S.), THoffmann@atb-potsdam.de (T.H.)
[7] HTW-Berlin, Treskowallee 8, 10318 Berlin, Germany; jonatan-bremer-berlin@web.de (S.J.B.)
* Correspondence: machado@ufpa.br; Phone.: +55-91-984-620325

**Abstract:** In this work, the effect of reaction time and biomass-to-$H_2O$ ratio on the structural evolution of hydro-char and kinetic of by hydrothermal processing of corn Stover with hot compressed $H_2O$, have been systematically investigated. The experiments were carried out at 250 °C, heating rate of 2.0 °C/min, biomass-to-$H_2O$ ratio of 1:10, and reaction times of 60, 120, and 240 minutes, and at 250 °C, 240 minutes, heating rate of 2.0 °C/min, and biomass-to-$H_2O$ water ratio of 1:10, 1:15, and 1:20, using a pilot scale stirred tank reactor of 5 gallon. The characterization of solid phase products performed by thermo-gravimetric analysis, scanning electron microscope, energy dispersive X-ray spectroscopy, X-ray diffraction, and elemental analysis (C, N, H, S). The physical-chemistry properties of solid phase analyzed in terms of dry matter (DM), total organic content (TOC), and ash. The yields of solid and gas phases decrease linearly with decreasing biomass-to-$H_2O$ ratio, while that of liquid phases increases linearly. For constant biomass-to-$H_2O$ ratio, the yields of solid, liquid, and gaseous reaction products varied between 52.97 and 35.82% (wt.), 44.84 and 54.59% (wt.), and 2.19 and 9.58% (wt.), respectively. The yield of solids decreases exponentially by decreasing the reaction time, while the yields of liquid and gas phases increase exponentially. For constant biomass-to-$H_2O$ ratio, TG/DTG curves shows that reaction time of 60 minutes was not enough to carbonize corn Stover. For constant reaction time, TG/DTG curves shows that increasing the $H_2O$-to-biomass ratio worse the carbonization of corn Stover. For constant biomass-to-$H_2O$ ratio, the SEM images show the main morphological structure of the corn Stover remains practically unchanged, while for constant reaction time, SEM images show that plant microstructure retains part of its original morphology, demonstrating that a decrease on biomass-to-$H_2O$ ratio worse the carbonization of corn Stover. For constant biomass-to-$H_2O$ ratio, the EDX analysis shows that the carbon content in hydro-char increases with reaction time, while for constant reaction time, the carbon content decreases with increasing biomass-to-$H_2O$ ratio. The kinetic of corn Stover degradation was correlated

 doi:10.20944/preprints202211.0402.v1



with a pseudo-first order exponential model, exhibiting a root-mean-square error ($r^2$) of 1.000, demonstrating that degradation kinetics of corn Stover with hot compressed $H_2O$, expressed as hydro-char formation, is well described by an exponential decay kinetics.

**Keywords:** Corn Stover; Hydrothermal carbonization; Hydro-char characterization; Kinetics of major compounds; Structural evolution

## 1. Introduction

Corn Stover is considered an agricultural waste, usually incinerated or used as bedding in poultry farms in Brazilian rural properties, being a lignocellulosic-base material abundant, but little used to generate income [1]. It is a residue left after harvesting of corn grains, consisting approximately of 25% (wt.) a leafy fraction (leaf + husk + sheaths) and between 70 and 75% (wt.) of fibrous and hard material (stalk + cobs) [2]. Brazil stands out as the third largest producer (101.14 million tons), behind China (260.96 million) and the USA. (347.05 million) [3]. In this context, just as tons of corn are produced, tons of agricultural waste are discarded [4], being a potential lignocellulosic-base residue for use, after submitted to hydrothermal processing [5-6], into a carbonaceous material with bio-adsorbent properties [5, 7].

The hydrothermal carbonization of lignin–cellulose-base materials including agricultural waste residues, such as corn Stover, with hot compressed $H_2O$ in the sub-critical is a thermo-chemical process of great potential [6-17], and the literature reports some studies on the hydrothermal carbonization of corn residues [5-6, 11, 14, 16-27], such as Stover [5-6, 14, 17-19, 21-25], corn Stalk [20], corn Silage [11], and until corn Stover activated with surfactant (Tween80, Span80, sodium dodecyl-benzenesulfonate, sodium lignosulfonate, PEG 400) [26], and corn Stover activated with KOH [27].

The influence of process parameters on hydrothermal carbonization including temperature, reaction time, and biomass-to-$H_2O$ ratio, as well as raw material characteristics on the yield of reaction products (solid, liquid, and gas) and chemical composition were systematically investigated by applying statistical methods to a huge collection of experimental data by Li *et al.* [28].

Li *et al.* [28] reported that the most analyzed product parameter by hydrothermal carbonization was hydro-char yield, while less attention has been given to the chemical composition of aqueous phase [6, 9, 12, 14-15, 24, 29-35], reaction time [20, 24, 34-60], kinetics of hydro-char conversion [37-41], and structural evolution of hydro-char [43-44, 61-66]. In addition, the excellent reviews of hydrothermal carbonization reaction mechanism by Funke & Ziegler [8], hydro-char properties design and applications of hydrothermal carbonization by Román *et al.* [67], applications of hydrothermal carbonization on energy and environment by Maniscalco *et al.* [68], structural characterization of hydrothermal carbonization hydro-char by Nizamuddin *et al.* [69], and chemistry, processes and applications of wet pyrolysis by Libra *et al.* [70], emphasizes the effect of process parameters including temperature, reaction time, biomass-to-$H_2O$ ratio on hydro-char yield, kinetics of hydro-char conversion, and structural evolution of hydro-char [11, 67-70], corroborated by the statistical analysis performed by Li *et al.* [28]. *However, until the moment no study has simultaneously investigate the structural evolution of hydro-char, the kinetic of hydro-char conversion*.

The effect of reaction time by hydrothermal carbonization, a process parameter affecting not only the yield of hydro-char, but also its morphological, crystalline, textural properties, has been also investigated in the last years [20, 24, 34-60]. Despite a considerable number of studies on the effect of reaction time by hydrothermal carbonization, only as few studies investigated the kinetics of hydro-char conversion [37-41], and the kinetics of structural evolution [43, 61-60, 64-65].

 doi:10.20944/preprints202211.0402.v1



The influence of biomass-to-$H_2O$ ratio by hydrothermal carbonization, a process variable affecting the physical-chemical properties of reaction products, including the yield of hydro-char, but also its morphological, crystalline, textural properties, has been also investigated in the last years [20-21,34,36,40,44-46,48-49,50,52,56-57,61-62]. Despite the large number of studies on the effect of biomass-to-$H_2O$ ratio by hydrothermal carbonization, only as few studies investigated the effects of this process parameter on the characteristics of hydro-char [61,65], particularly on the structural evolution [61,65].

The effects of process parameters on the structural evolution of hydro-chars such as temperature [6,14-15,29-30,38,41,63], reaction time [20, 24, 34-60], and biomass-to-$H_2O$ ratio by hydrothermal carbonization [20-21,34,36,40,44-46,48-49,50,52,56-57,61-62], may cause drastic changes on the physical-chemical properties of reaction products, including the yield of hydro-char, composition of aqueous phase, composition of gaseous phase, and morphological, crystalline, textural properties of hydro-char, has been also investigated in the last years [6,14-15,20-21,29-30,34-63]. In this context, *this study aims to simultaneously investigate the structural evolution of hydro-char, the kinetic of hydro-char conversion.*

In this work, the effect of reaction time and biomass-to-$H_2O$ ratio on the structural evolution of hydro-char by analyzing its morphological, crystalline, and textural properties, as well as kinetic of corn Stover degradation by hydrothermal processing of corn Stover with hot compressed $H_2O$, have been systematically investigated at 250 °C, heating rate of 2.0 °C/min, biomass-to-$H_2O$ ratio of 1:10, and reaction times of 60, 120, and 240 minutes, and at 250 °C, 240 minutes, heating rate of 2.0 °C/min, and biomass-to-$H_2O$ water ratio of 1:10, 1:15, and 1:20, using a pilot scale stirred tank reactor of 5 gallon. The novelty of this work remains on the innovative way of analyzing simultaneously *the structural evolution of hydro-char (elemental analysis, scanning electron microscopy, thermal gravimetric analysis, energy-dispersive x-ray spectroscopy, x-ray diffraction), the kinetic of hydro-char conversion, and modeling of hydro-char conversion kinetics as a function of reaction time and biomass-to-$H_2O$ ratio, using a pilot scale stirred tank reactor of 5 gallon.*

## 2. Materials and Methods

### *2.1. Methodology*

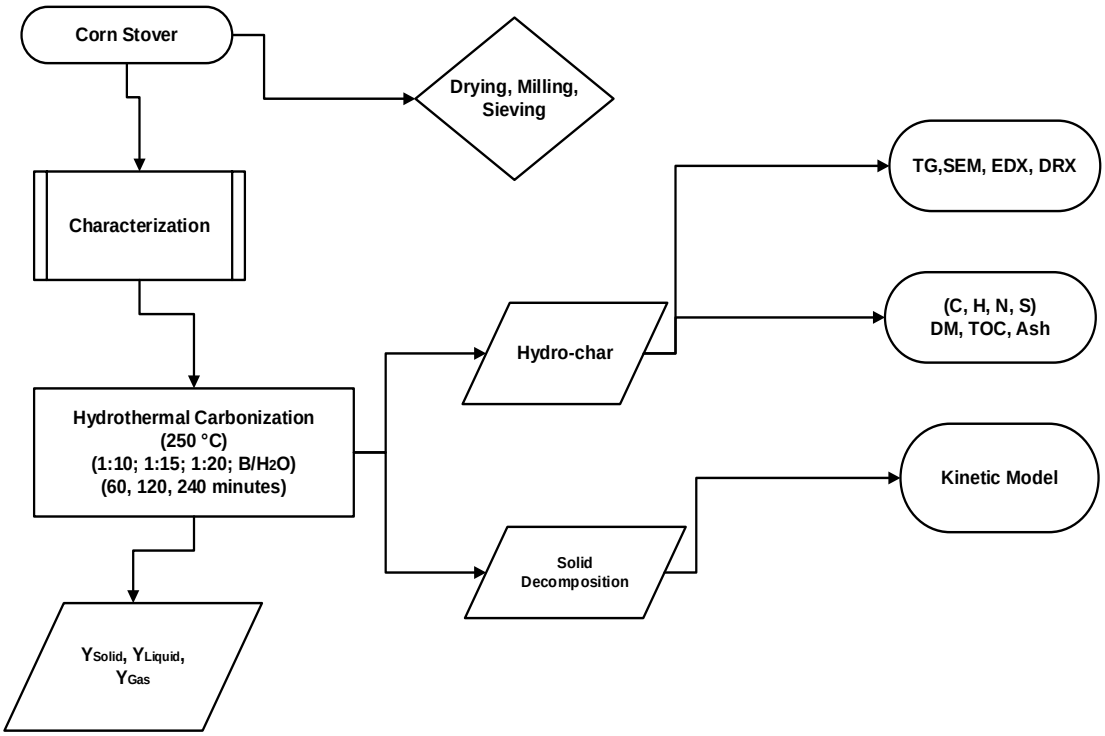


**Figure 1.** Process flow sheet by hydrothermal processing of corn Stover with hot compressed $H_2O$ at 250 °C, biomass-to-$H_2O$ ratio of 1:10, 60, 120, and 240 min, 250 °C, 240 min, and biomass-to-water ratios of 1:10, 1:15, and 1:20, in pilot scale.

 doi:10.20944/preprints202211.0402.v1



The process flow sheet shown in Figure 1 summarizes the applied methodology, described in a logical sequence of ideas, chemical methods, and procedures by hydrothermal processing of corn Stover with hot compressed $H_2O$ at 250 °C, biomass-to-$H_2O$ ratio of 1:10, 60, 120, and 240 minutes, and at 250 °C, 240 minutes, and biomass-to-$H_2O$ ratios of 1:10, 1:15, and 1:20, in pilot scale. Initially, the corn Stover residues are collected. Afterwards, subjected to pretreatments of drying, followed by milling and sieving. The experiments carried out in pilot scales to investigate the effect of process time (60, 120, and 240 minutes) and biomass-to-$H_2O$ ratio (1:10, 1:15, 1:20) on structural evolution of solid phase products, yields of hydro-char, $H_2O$, and gas, and kinetics of corn Stover degradation. The solid phase product characterized by TG/DTG, SEM, EDX, and XRD.

*2.2. Materials, pre-treatment, and characterization of corn Stover*

The corn Stover residues used was provided by Leibniz-Institüt für Agrartechnik und Bioökonomie e.V (ATB), Potsdam-Bornin [5-6]. The corn Stover residues were submitted to the pre-treatments of drying at 105 °C using a digital controlled oven, grinding using a laboratory cutting mill, and finally sieved to produce particle sizes averaging 2.0 mm of square geometry, as described in the literature [5-6]. The hydro-chars physicochemical characterized for dry matter, total organic content, ash content, elemental analysis (C, H, N, and S), and oxygen content, as described elsewhere [5-6].

*2.3. Experimental apparatus and procedures*

The pilot-scale reactor of cylindrical geometry ($V_{Reactor}$ = 18.875 L), described in details elsewhere [5-6,15], constructed by stainless steel (Parr, USA, Model: 4555), includes a mechanical stirring system with 02 impellers, each containing 3-blades, and 6.78 N.m Torque. The reactor has a ceramic-3 zone heater of 4500 W, and a control unit (Parr, USA, Model: 4848). The temperature is measured with aid 02 thermocouples placed inside a thermos well. The reactor operates at a maximum pressure of 131 bar and maximum temperature of 350 °C. The hydrothermal processing of dried corn Stover was carried out with hot compressed water at 250 °C, 240 min, and biomass-to-water ratios of 1:10, 1:15, and 1:20, and at 250 °C, biomass-to-water ratio of 1:10, and 60, 120, and 240 min, as described in details in the literature [5-6,15]. For the experiments with varying biomass/$H_2O$ ratio, 600 g of corn Stover residues were placed inside the reactor. Afterwards, 6000, 9000 and/or 12000 g $H_2O$, depending on the biomass/$H_2O$ ratio, were inserted within the reactor and soaked manually until an homogeneous cake is formed and reactor sealed. The operating temperature and the heating rate set at 250 °C and 2.0 °C/min, respectively. The reaction times start at the point the reactor reaches the set point temperature ($\tau_0$). Once the reaction time is reached for each batch (60, 120 and/or 240 min), the reactor is cooled down until ambient temperature. The gravitational dewatering makes it possible to separate the liquid and solid phases. The moist solid phase inside the reactor is removed and placed inside a mechanical press to remove the residual water. Afterwards, the solid and aqueous phases determined gravimetrically. The moist solid phase is dried at 105 °C for 48 h to determine the moist content. Samples of moist dewatered solids, liquid phase, and dried solid phase stored for physicochemical analysis and morphological characterization.

*2.4. Physicochemical analysis and characterization of solid phase products*

*2.4.1. Physicochemical analysis of solid phase*

The hydro-char characterized for dry matter, ash content, and elemental analysis (C, H, N, and S) [5-6,15].

*2.4.2. Characterization of hydro-char*

The morphological, crystalline, and thermogravimetric characterization was performed by thermo-gravimetric analysis (TG/DTG), scanning electron microscope (SEM), energy dispersive X-ray spectroscopy (EDX), and X-ray diffraction (XRD), described in details elsewhere [5,7].

Preprints (www.preprints.org) | NOT PEER-REVIEWED | Posted: 22 November 2022 doi:10.20944/preprints202211.0402.v1



*2.5. Material balances and yields of reaction products*

The law of conservation of mass was applied within the reactor, operating as a closed thermodynamic system, batch mode, yielding the following equations.

$$M_{Reactor} = M_{Feed} \quad (1)$$

$$M_{Reactor} = M_{Solid} + M_{LP} + M_{Gas} \quad (2)$$

Where $M_{Reactor}$ is the mass of reactor, $M_{Feed} = M_{Corn\ Stover}$ is the mass of corn Stover filled into the reactor, $M_{Solid}$ is the mass of hydro-char, $M_{LP}$ is the mass of liquid phase products, and $M_{Gas}$ is the mass of gas. The process performance evaluated by computing the yields of liquid and liquid reaction products defined by equations (3) and (4), and the yield of gas by difference, using equation (5).

$$Y_{LP}[\%] = \frac{M_{LP}}{M_{Corn\ Stover}} x100 \quad (3)$$

$$Y_{Solid}[\%] = \frac{M_{Solid}}{M_{Corn\ Stover(0)}} x100 \quad (4)$$

$$Y_{Gas}[\%] = 100 - (Y_{LP} + Y_{Solid}) \quad (5)$$

*2.7. Degradation kinetics of corn Stover*

The degradation kinetics of corn Stover by hydrothermal processing at 250 °C, biomass-to-$H_2O$ ratio of 1:10, 60, 120 and 240 min, expressed as hydro-char formation, was correlated with a pseudo-first order exponential model [41].

The thermal degradation process of biomass, in this case, corn Stover, follows the idea and/or concept of Yin *et. al.* [41].

By performing a mass balance on the dry biomass, at the beginning, the mass of biomass is equal the mass of solids

$$M_{Biomass}(0) = M_{Corn\ Stover}(0) = M_{Solids}(0) \quad (6)$$

$$M_{Biomass}(0) = M_{Gas}(\tau) + M_{Liquids}(\tau) + M_{Solids}(\tau) \quad (7)$$

By considering that

$$M_{Dissolution}(\tau) = M_{Gas}(\tau) + M_{Liquids}(\tau) \quad (8)$$

The initial mass of biomass, $M_{Biomass}(0)$, is equal to the sum of the mass of solids and the mass of dissolution at time τ, $M_{Dissolution}(\tau) + M_{Solids}(\tau)$.

$$M_{Biomass}(0) = M_{Dissolution}(\tau) + M_{Solids}(\tau) \quad (9)$$

The time differential of equation (9) is given as follows:

$$\frac{dM_{Solids}(\tau)}{d\tau} = -\frac{dM_{Dissolution}(\tau)}{d\tau} \quad (10)$$

Assuming the mass of solid phase products is equal to the mass of hydro-char yields equation (11).

$$M_{Solids}(\tau) = M_{Hydrochar}(\tau) \quad (11)$$

The time differential of equation (11) is given as follows:

$$\frac{dM_{Solids}(\tau)}{d\tau} = \frac{dM_{Hydrochar}(\tau)}{d\tau} \quad (12)$$

The biomass dissolution was described by a modified first order kinetics given by equation (13).

$$\frac{dM_{Solids}(\tau)}{d\tau} = -K * [M_{Solids}(\tau) - a] \quad (13)$$

Dividing equation (13) by equation (6) yields equation (14).

$$\frac{d[M_{Solids}(\tau)/M_{Solids}(0)]}{d\tau} = -K * [Y_{Solids}(\tau) - A] \quad (14)$$

$$\frac{dY_{Solids}(\tau)}{d\tau} = -K * [Y_{Solids}(\tau) - A] \quad (15)$$

The constant A, defined as $a/M_{Solids}(0)$, is included as a correction term. By solving the 1st order homogeneous and linear differential equation (15), with initial boundary condition, $\tau = 0, Y_{Solids}(\tau) = Y_{Solids}(0)$, yields equation (16).

$$Y_{Solids}(\tau) = A + [Y_{Solids}(0) - A] * \exp(-K * \tau) \quad (16)$$

Preprints (www.preprints.org) | NOT PEER-REVIEWED | Posted: 22 November 2022 doi:10.20944/preprints202211.0402.v1



## 3. Results

### *3.1. Thermogravimetric, morphological and mineralogical characterization of hydro-char*

#### *3.1.1 Thermo-gravimetric analysis (TG/DTG)*

*3.1.1.1 Influence of reaction time*

The thermal degradation of corn Stover was analyzed via thermogravimetric analysis (TG/DTG) by Sittisun *et. al.* [71], between 25 and 900 °C, heating rates of 10, 20, and 50 °C/min, as well as by Mohammed *et al.* [21], between 25 and 600 °C, heating rates of 10 °C/min. For heating rates of 10 °C/min, Sittisun *et. al.* [71], reported mass loss of 92% (wt.), within the temperature interval of 25 and 510 °C, while Mohammed *et al.* [21], reported mass loss of ≈ 70.0% (wt.), between 25 and 600 °C. Sittisun *et. al.* [71], reported the occurrence of 03 (three) degradation steps, the first between 25 and 167 °C, due to removal of moisture, a second between 167 and 368 °C, due to removal of volatile compounds by degradation of hemi-cellulose and cellulose, and a third between 368 and 514 °C, due to thermal degradation and/or combustion of lignin [71]. Mohammed *et al.* [21], also reported the occurrence of 03 (three) disintegration steps, the first between 100 and 250 °C, due to removal of moisture and some volatiles, a second between 250 and 400 °C, due to the degradation of hemi-cellulose and cellulose, and a third above 450 °C, due to thermal degradation of lignin [21]. The thermal degradation of bio-char obtained by hydrothermal processing of corn Stover at 250 °C, 240 min, 1:10 biomass-to-$H_2O$ ratio, using a reactor of 18.927 L, was analyzed via thermogravimetric analysis (TG/DTG) by Costa *et. al.* [7], between 25 and 800 °C, 10 °C/min, under $N_2$ atmosphere, as well as by Mohammed *et al.* [21], between 25 and 600 °C, 10 °C/min, under $N_2$ atmosphere.

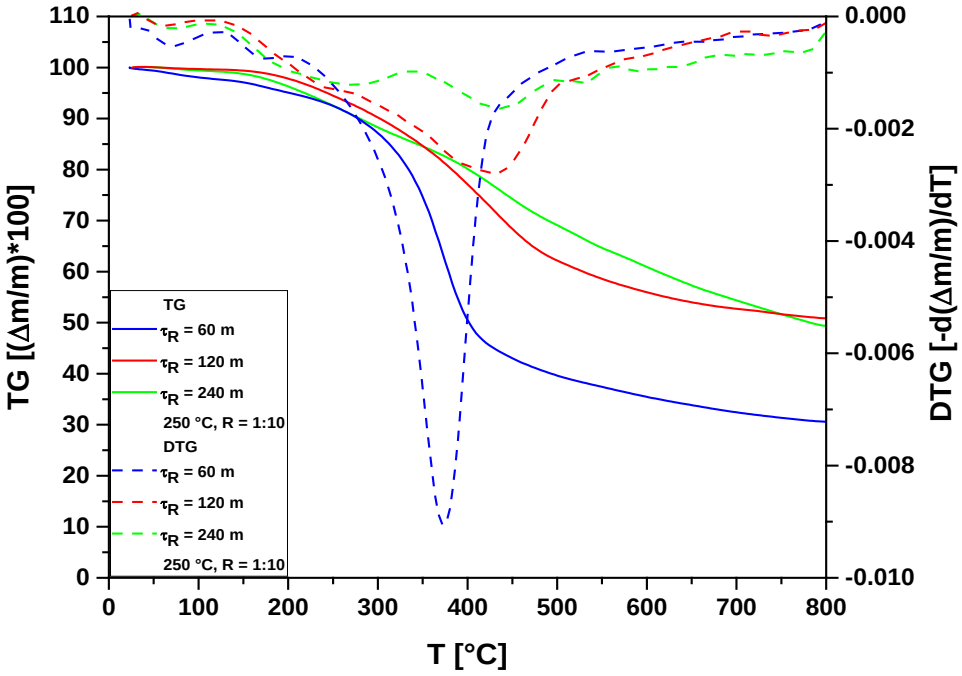


Figure 2. TG/DTG of hydro-chars obtained by hydrothermal processing of corn Stover at 250°C, biomass/$H_2O$ ratio of 1:10, 60, 120, and 240 minutes, using a reactor of 18.927 L.

Figure 2 illustrates the TG/DTG of hydro-chars obtained by hydrothermal processing of corn Stover at 250°C, biomass/$H_2O$ ratio of 1:10, 60, 120, and 240 minutes, using a reactor of 18.927 L. One observes the presence of 03 (three) reaction steps, being according to the similar results reported in the literature [7,21]. The TG/DTG curves for the hydro-chars obtained at 240 and 120 minutes by hydrothermal processing of corn Stover at 250 °C, 1:10

Preprints (www.preprints.org) | NOT PEER-REVIEWED | Posted: 22 November 2022 doi:10.20944/preprints202211.0402.v1



biomass-to-$H_2O$ ratio, using a reactor of 18.927 L, are identical, showing mass losses between 50.63 and 49.15% (wt.) for the temperature interval 25-800 °C. On the other hand, the TG/DTG curves for the hydro-chars obtained at 60 minutes by hydrothermal processing of corn Stover at 250 °C, 1:10 biomass-to-$H_2O$ ratio, using a reactor of 18.927 L, has a mass loss of 69.40% (wt.) for the temperature interval 25-800 °C, *showing that reaction time of 60 minutes was not enough to carbonize corn Stover*.

By the TG/DTG curves for the hydro-chars obtained at 60 and 120 minutes by hydrothermal processing of corn Stover at 250 °C, 1:10 biomass-to-$H_2O$ ratio, using a reactor of 18.927 L, it can be seen at the beginning, a small loss of mass around 100 °C, associated to the presence of water in hydro-chars. A mass loss of approximately 37.5% (wt.) was observed for the hydro-char obtained at 120 minutes by hydrothermal processing of corn Stover at 250 °C, 1:10 biomass-to-$H_2O$ ratio, between 204 and 530 °C, while for the hydro-char obtained at 60 minutes the mass loss was around 57.6% (wt.), between 159 to 506°C. These mass losses are possibly associated with the presence of volatile material produced by thermal degradation of lignocellulosic material (hemicellulose or cellulose). In addition, the temperature of peaks by DTG curve increase in line with increasing reaction time, showing that an increase in reaction time contributes to the formation of more stable compounds.

*3.1.1.2 Influence of biomass-to-$H_2O$ ratio*

The thermal degradation (TG/DTG) of hydro-char obtained by hydrothermal processing of corn Stover at 250 °C, 240 min, biomass-to-$H_2O$ ratio of 1:10, 1:15, and 1:20, using a reactor of 18.927 L, between 25 and 800 °C, 10 °C/min, under $N_2$ atmosphere, is shown in Figure 3.

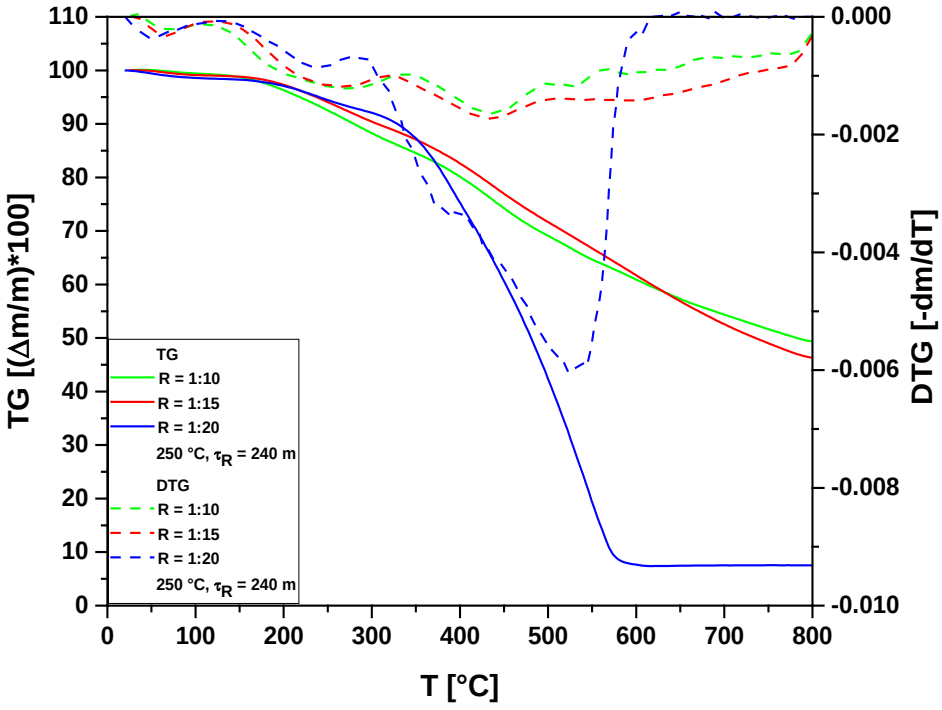


Figure 3. TG/DTG of hydro-chars obtained by hydrothermal processing of corn Stover at 250°C, 240 min, biomass/$H_2O$ ratio of 1:10, 1:15, and 1:20, using a reactor of 18.927 L.

The TG/DTG curves for biomas-to-$H_2O$ ratios of 1:10 and 1:15 are identical, showing mass losses between 50.63 and 53.68% (wt.), respectively. However, if one decreases the biomas-to-$H_2O$ ratio of 1:15 to 1:20, the mass loss increases from 53.68 to 92.48% (wt.), showing a decrease on the carbonization grade of hydro-char, *that is, biomas-to-$H_2O$ ratio of 1:20 time of 60 minutes was not enough to carbonize corn Stover*. This is according to the

 doi:10.20944/preprints202211.0402.v1



literature [15,72-73], as an increase on the $H_2O$-to-biomass ratio favors the hydrolysis reactions by hydrothermal processing of lign-cellulosic materials. As cellulose hydrolyzes, glucose is produced, being transformed into fructose [74]. The hydrothermal decomposition of fructose produces low carbon chain carboxylic acids, dissociating within the aqueous phase, producing $H_3O^+$. By increasing the $H_2O$-to-biomass ratio, a decrease on the concentration of volatile carboxylic acids, particularly acetic acid, within the aqueous phase is expected; causing a diminution on the ionic product of aqueous phase, worsen the degradation process of biomass [74]. By the hydrothermal processing of Açaí seeds with hot compressed $H_2O$ at 250 °C, heating rate of 2 °C/min, 240 min, da Silva *et. al.* [15], stated that hydrolysis is probably the dominant reaction mechanism, but not the only one, as the $H_2O$-to-biomass ratio increases from 1:10 to 1:20. Figure 3 shows for hydro-char obtained at 250 °C, 60 min, biomass-to-$H_2O$ ratio of 1:20, a mass loss of 92.48% (wt.), proving that most of hemi-cellulose, cellulose and lignin were not thermally degraded. This is corroborated for the peaks by DTG curve at 390 °C and 525 °C, respectively, characteristics of hemi-cellulose/cellulose and lignin degradation, showing that an increase in $H_2O$-to-biomass ratio worse the carbonization of corn Stover by hydrothermal processing, as most of hemi-cellulose and cellulose still retains its structure.

### *3.1.2 Scanning electron microscopy*

The SEM analysis performed to investigate the effect of reaction time and biomass/$H_2O$ ratio on the evolution and/or changes on the microstructure of corn Stover after hydrothermal processing with hot compressed $H_2O$, as illustrated in details in Supplementary Figures S1-S13.

*3.1.2.1 Influence of reaction time*

The microscopies of bio-char obtained by hydrothermal processing of corn Stover at 250°C, biomass/$H_2O$ ratio of 1:10, and 60 minutes, using a reactor of 18.927 L, shown in Figure 4. By the SEM images illustrated in Figures 4a, 4b and 4c, at different magnifications [MAG: 200× (**a**); MAG: 1000× (**b**); MAG: 5000× (**c**)], one observes the rupture of polymer bundles (fibers) and opening of pores in the cellular tissue, showing that fragmentation of hemi-cellulose and cellulose begins [75]. However, the main morphological structure of the corn Stover remains practically unchanged, since the plant microstructure retains its characteristics, *demonstrating that reaction time of 60 minutes was not enough to carbonize corn Stover, as described in section 3.1.1.1.* The results are according to similar studies on the influence of reaction time over the morphology of hydro-chars reported in the literature [21,24,54,62,65].

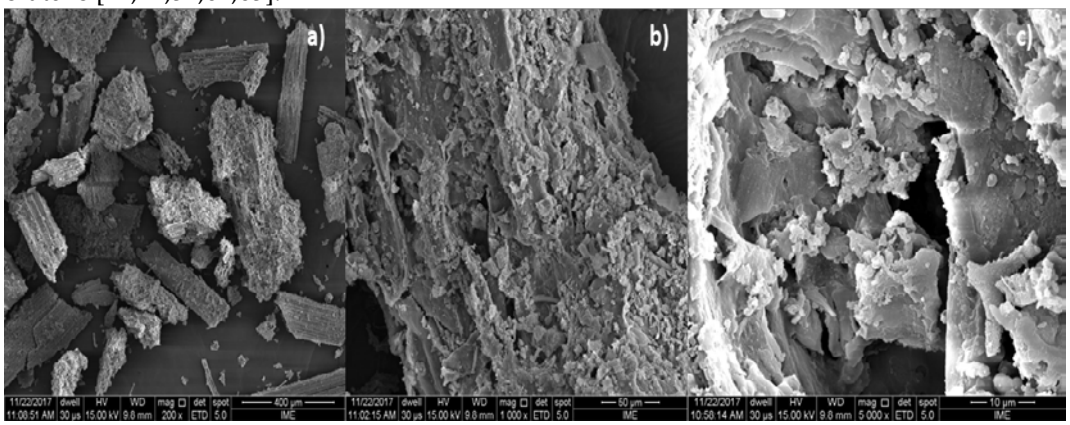


Figure 4. SEM of hydro-chars obtained by hydrothermal processing of corn Stover at 250°C, biomass/$H_2O$ ratio of 1:10, and 60 minutes [MAG: 200× (**a**); MAG: 1000× (**b**); MAG: 5000× (**c**)].

Figure 5 shows the SEM microscopies of bio-char obtained by hydrothermal processing of corn Stover at 250°C, biomass/$H_2O$ ratio of 1:10, and 120 minutes, using a reactor of 18.927 L.

Preprints (www.preprints.org) | NOT PEER-REVIEWED | Posted: 22 November 2022 doi:10.20944/preprints202211.0402.v1



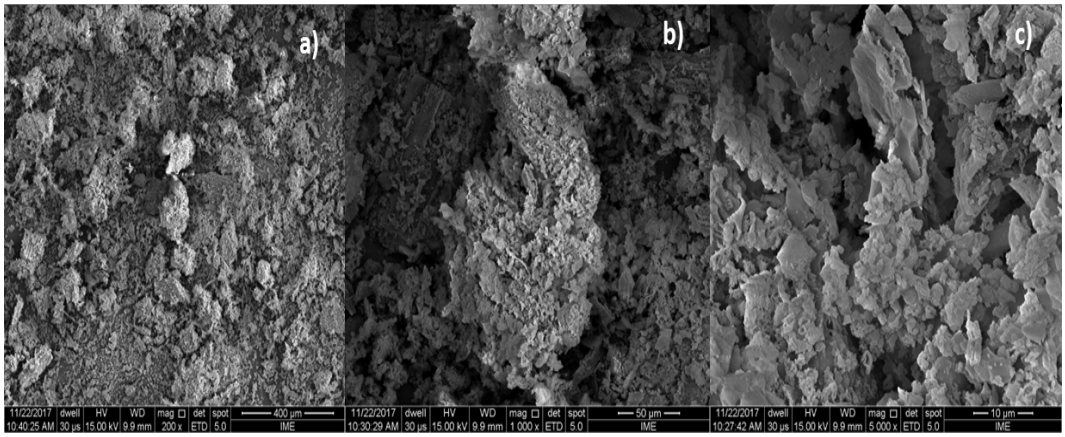


Figure 5. SEM of hydro-chars obtained by hydrothermal processing of corn Stover at 250°C, biomass/$H_2O$ ratio of 1:10, 120 minutes [MAG: 200× (**a**); MAG: 1000× (**b**); MAG: 5000× (**c**)].

The scanning electron microscopies at different magnifications illustrated in Figure 5 [MAG: 200× (**a**); MAG: 1000× (**b**); MAG: 5000× (**c**)], show that the morphological microstructure of corn Stover has been drastically changed, as the fibers of plant tissue were destroyed by fragmentation of hemi-cellulose and cellulose [74], and the pores on the vegetal tissue are open. In addition, Figure 5c shows the appearance of microspheres, which is according to the results reported by Xing *et al.* [74]. The plant microstructure retains no longer its original morphology, *demonstrating that reaction time of 120 was able to carbonize corn Stover, as described in section 3.1.1.1.*

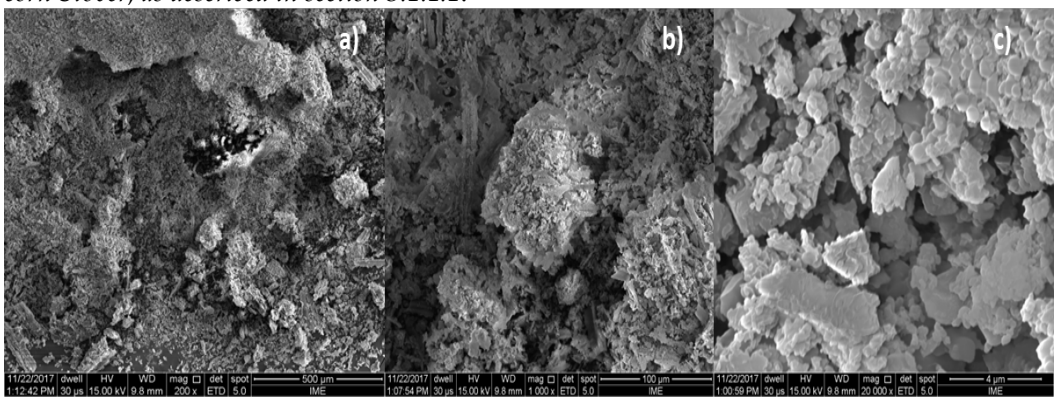


Figure 6. SEM of hydro-chars obtained by hydrothermal processing of corn Stover at 250°C, biomass/$H_2O$ ratio of 1:10, 240 minutes, using a reactor of 18.927 L [MAG: 200× (**a**); MAG: 1000× (**b**); MAG: 20,000× (**c**)].

The microscopies of bio-char obtained by hydrothermal processing of corn Stover at 250°C, biomass/$H_2O$ ratio of 1:10, and 240 minutes, using a reactor of 18.927 L, shown in Figure 6. The SEM images illustrated in Figures 6a, 6b and 6c, at different magnifications [MAG: 200× (**a**); MAG: 1000× (**b**); MAG: 20,000× (**c**)], show that the microstructure of corn Stover has been destroyed due to fragmentation of hemi-cellulose and cellulose [7,74]. The cellular tissue replaced by an aggregate amorphous solid consisting of a layer of microspheres [7], *demonstrating that reaction time of 240 was able to carbonize corn Stover, as described in section 3.1.1.1.* The results are according to similar studies on the influence of reaction time over the morphology of hydro-chars reported in the literature [21,24,54,62,65].

*3.1.2.1 Influence of biomass-to-$H_2O$ ratio*

The microscopies of bio-char obtained by hydrothermal processing of corn Stover at 250°C, biomass/$H_2O$ ratio of 1:15, and 240 minutes, using a reactor of 18.927 L, shown in Figure 7. da Silva *et al.* [15], investigated the effect of biomass-to-$H_2O$ ratio on the hydrothermal processing of Açaí seeds, stating that an increase on the $H_2O$-to-biomass ratio enhances the hydrolysis of cellulose.

Preprints (www.preprints.org) | NOT PEER-REVIEWED | Posted: 22 November 2022 doi:10.20944/preprints202211.0402.v1



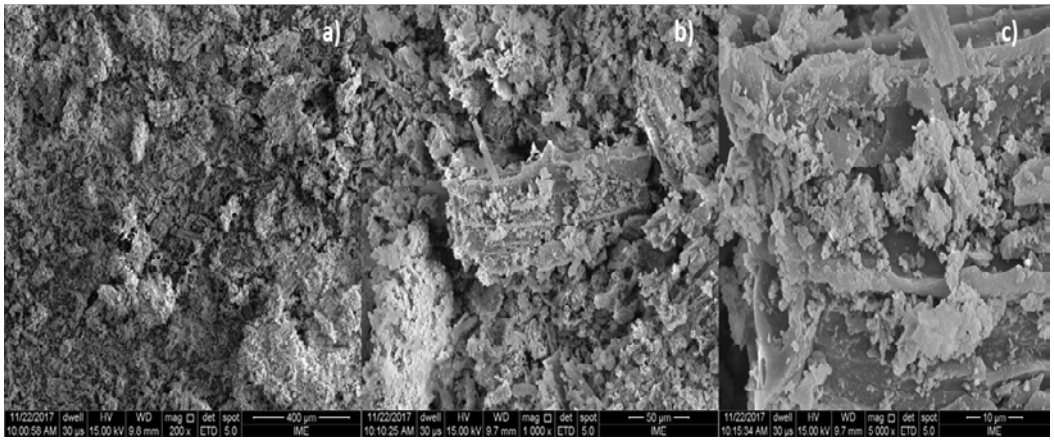


Figure 7. SEM of hydro-chars obtained by hydrothermal processing of corn Stover at 250°C, biomass/$H_2O$ ratio of 1:15, 240 minutes, using a reactor of 18.927 L [MAG: 200× (**a**); MAG: 1000× (**b**); MAG: 5000× (**c**)].

The SEM images, at different magnifications [MAG: 200× (**a**); MAG: 1000× (**b**); MAG: 5000× (**c**)], show that the microstructure of corn Stover has been changed, as the pores on the vegetal tissue are open, probably due to hydrolysis reaction of cellulose and hemi-cellulose, as reported by da Silva et al [74]. However, by increasing the magnification 5000×, as shown in Figure 7c, one observes that rupture of polymer bundles (fibers) and opening of pores in the cellular tissue was not so effective to change the microstructure of corn Stover. The plant microstructure retains part of its original morphology, *demonstrating that a decrease on biomass-to-$H_2O$ ratio worse the carbonization of corn Stover*.

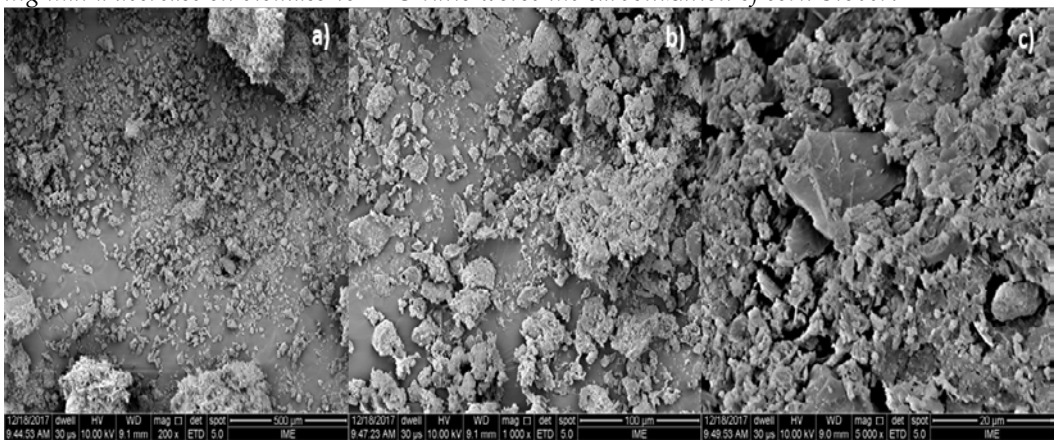


Figure 8. SEM of hydro-chars obtained by hydrothermal processing of corn Stover at 250°C, biomass/$H_2O$ ratio of 1:20, 240 minutes [MAG: 200× (**a**); MAG: 1000× (**b**); MAG: 5000× (**c**)].

The microscopies of bio-char obtained by hydrothermal processing of corn Stover at 250°C, biomass/$H_2O$ ratio of 1:20, and 240 minutes, using a reactor of 18.927 L, at different magnifications [MAG: 200× (**a**); MAG: 1000× (**b**); MAG: 5000× (**c**)], shown in Figure 8. The SEM image at a magnification of 5000×, illustrated in Figure 8c, shows that microstructure of corn Stover retains its original characteristics, that is, the morphology of corn Stover remains practically unchanged, *demonstrating that higher $H_2O$-to-biomass ratio worse the carbonization of corn Stover* as hydrolysis reactions of cellulose and hemi-cellulose are the major degradation mechanism [15].

### *3.1.3* Energy Dispersive X-ray Spectroscopy

Table 1 shows the EDX analysis of hydro-chars obtained by hydrothermal processing of corn Stover with hot compressed $H_2O$ at 250°C, biomass/$H_2O$ ratio of 1:10, 60, 120, and 240 minutes, and at 250°C, 240 minutes, and biomass-to-$H_2O$ ratio of 1:10, 1:15, and 1:20, using a reactor of 18.927 L. The results show that carbon content increases with increasing reaction time between 60 and 120 minutes, being according to the results presented in

 doi:10.20944/preprints202211.0402.v1



Figure 2 and Figures 4c, 5c, and 6c, while between 120 and 240 minutes the carbon content is almost identical. By decreasing the biomass-to-$H_2O$ ratio between 1:10 and 1:15, littlle variation on the carbon content of hydro-chars has been observerd, while a drastic decrease on the carbon content occurred between 1:15 and 1:20, *demonstrating that higher $H_2O$-to-biomass ratio worse the carbonization of corn Stover*. The energy dispersive x-ray spectroscopy (EDX) identified also the presence of Si, K, Ca, Mg, Al, S, and Fe. The micronutrients (Fe, Si), macronutrients (C, O, Ca, K, Mg, S), as well as heavy metals (Al) identified by EDX in hydro-chars are according to inorganics compounds identified in corn Stover after drying at 105 °C [76].

Table 1: Percentages in mass and atomic mass of hydro-char obtained by hydrothermal carbonization of corn Stover at 250 °C, 60, 120, and 240 minutes, biomass-to-water ratio of 1:10, and at 250 °C, 240 minutes, biomass-to-water ratio of 1:10, 1:15, and1:20, using a pilot scale reactor of reactor of 18.927 L.

| | **Hydro-char** | | | | | | | | | | | | | | |
|---|---|---|---|---|---|---|---|---|---|---|---|---|---|---|---|
| | **250 °C, biomass-to-$H_2O$ ratio of 1:10** | | | | | | | | | **250 °C, 240 minutes** | | | | | |
| | **60 [min]** | | | **120 [min]** | | | **240 [min]** | | | **1:15 [$g_{biomass}/g_{H2O}$]** | | | **1:20 [$g_{biomass}/g_{H2O}$]** | | |
| **CE** | **Mass [wt.%]** | **Atomic Mass [wt.%]** | **SD** | **Mass [wt.%]** | **Atomic Mass [wt.%]** | **SD** | **Mass [wt.%]** | **Atomic Mass [wt.%]** | **SD** | **Mass [wt.%]** | **Atomic Mass [wt.%]** | **SD** | **Mass [wt.%]** | **Atomic Mass [wt.%]** | **SD** |
| **C** | **43.76** | **74.14** | 3.14 | **50.15** | **84.94** | 3.59 | **58.65** | **85.11** | **4.26** | **76.04** | **81.05** | 0.631 | **6.04** | **28.01** | **0.70** |
| **O** | **16.29** | **20.72** | 1.33 | **6.91** | **8.79** | 0.68 | **11.03** | **12.02** | **1.01** | **23.59** | **18.87** | 0.632 | **5.58** | **19.41** | **0.63** |
| **Si** | 0.75 | 0.54 | 0.05 | 0.50 | 0.32 | 0.04 | - | - | - | - | - | - | 5.09 | 10.09 | 0.18 |
| **K** | 0.17 | 0.09 | 0.03 | 1.02 | 0.53 | 0.05 | - | - | - | - | - | - | - | - | - |
| **Ca** | 1.06 | 0.54 | 0.05 | 2.73 | 1.39 | 0.08 | 0.48 | 0.21 | 0.04 | - | - | - | 2.60 | 3.61 | 0.10 |
| **Mg** | - | - | - | - | - | - | - | - | - | - | - | - | 0.33 | 0.77 | 0.04 |
| **Al** | - | - | - | - | - | - | - | - | - | - | - | - | 2.48 | 5.12 | 0.11 |
| **S** | - | - | - | - | - | - | - | - | - | - | - | - | 0.87 | 1.51 | 0.05 |
| **Fe** | - | - | - | - | - | - | - | - | - | - | - | - | 13.35 | 13.31 | 0.56 |
| **Zn** | - | - | - | - | - | - | - | - | - | 0.366 | 0.072 | 0.065 | - | - | - |
| **Pt** | 37.97 | 3.96 | 0.87 | 38.69 | 4.03 | 0.90 | 29.84 | 2.67 | 0.76 | - | - | - | 63.66 | 18.17 | 1.72 |

**SD= Standard Deviation, CE= Chemical Elements**

### *3.1.4* X-ray diffraction

The x-ray diffraction of hydro-chars obtained by hydrothermal processing of corn stover with hot compressed $H_2O$ at 250°C, biomass/$H_2O$ ratio of 1:10, 60, 120, and 240 minutes, and at 250°C, 240 minutes, and biomass-to-$H_2O$ ratio of 1:10, 1:15, and 1:20, using a reactor of 18.927 L, are shown in Figure 9 and 10, respectively.

Preprints (www.preprints.org) | NOT PEER-REVIEWED | Posted: 22 November 2022 doi:10.20944/preprints202211.0402.v1



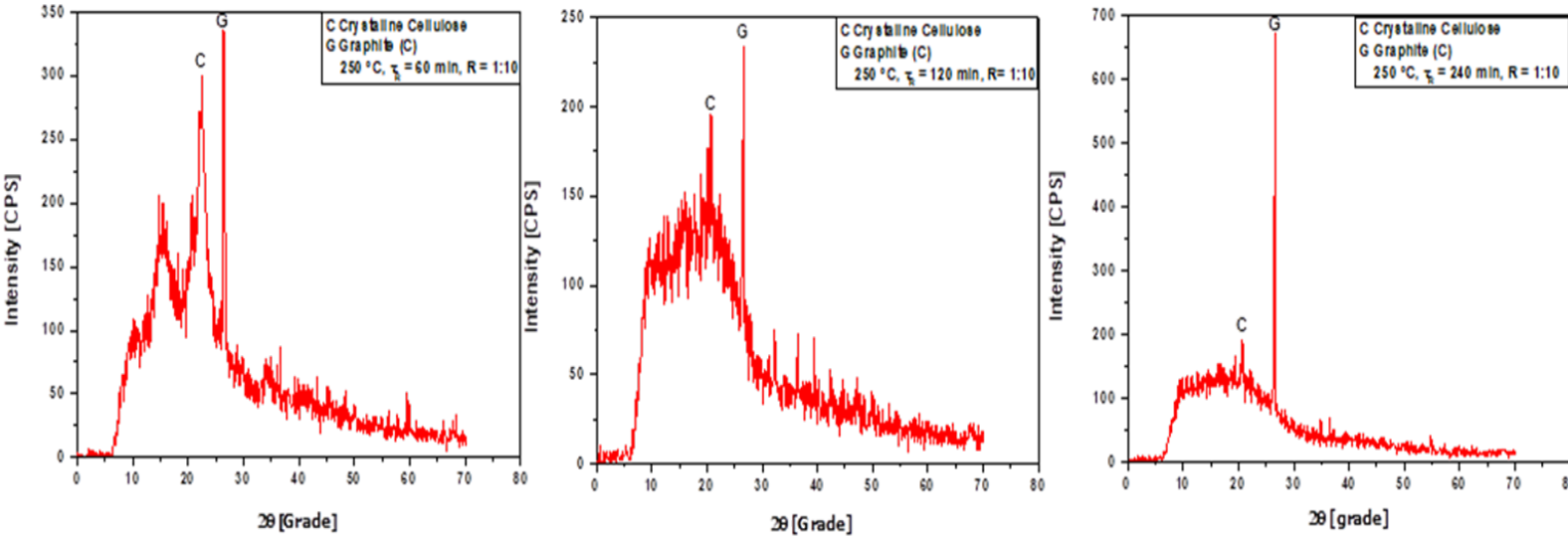


Figure 9. XRD of hydro-chars obtained by hydrothermal processing of corn Stover at 250°C, biomass/$H_2O$ ratio of 1:10, 60, 120 and 240 minutes, using a reactor of 18.927 L.

The diffractogram of hydro-chars illustrated in Figure 9 identified the presence of two crystalline phases-graphite (C) and crystalline cellulose. At 60 minutes, a peak of graphite of medium intensity (55.7%) was observed on the position 2θ: 26.47, and a peak of high intensity (100.0%), characteristic of crystalline cellulose [20, 77], on the position 2θ: 22.40. At 120 minutes, a peak of graphite of high intensity (100.0%) was observed on the position 2θ: 26.54, and a peak of high intensity (99.1%), characteristic of crystalline cellulose [20, 77], on the position 2θ: 22.73. At 240 minutes, a peak of graphite of high intensity (100.0%) was observed on the position 2θ: 26.47, and a peak of low intensity (12.95%), characteristic of crystalline cellulose [20, 77], on the position 2θ: 22.20. The results show the occurrence of peaks of higher intensity of graphite (C) as the reaction time succeeds.

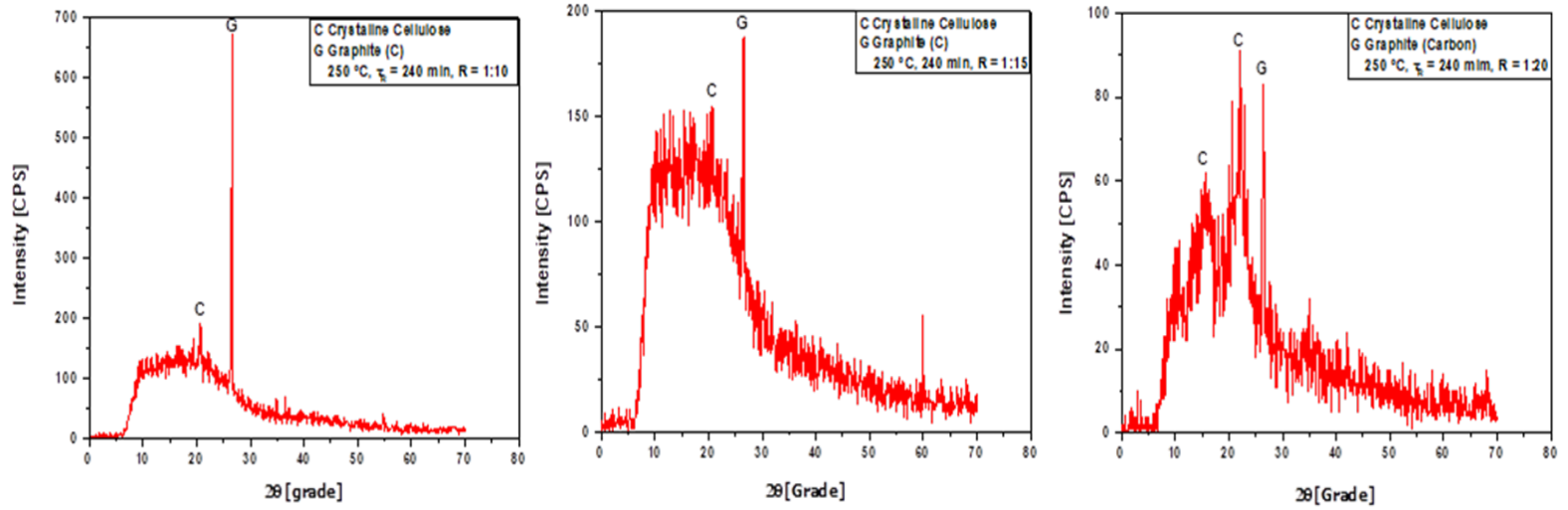


Figure 10. XRD of hydro-chars obtained by hydrothermal processing of corn Stover at 250°C, 240 minutes, biomass/$H_2O$ ratio of 1:10, 1:15, and 1:20, using a reactor of 18.927 L.

Figure 10 illustrates the XDR of hydro-chars obtained at 250°C, 240 minutes, and biomass-to-$H_2O$ ratio of 1:10, 1:15, and 1:20, using a reactor of 18.927 L. The diffractograms identified the presence of two crystalline phases—graphite (C) and crystalline cellulose. For biomass-to-$H_2O$ ratio of 1:10, a peak of graphite of high intensity (100.0%) was observed on the position 2θ: 26.47, and a peak characteristic of crystalline cellulose [20,77], of low intensity (12.95%), on the position 2θ: 22.20. For biomass-to-$H_2O$ ratio of 1:15, a peak of graphite of high intensity (100.0%) was observed on the position 2θ: 26.51, and a peak of low intensity, characteristic of crystalline cellulose [20,77], on the position 2θ:

Preprints (www.preprints.org) | NOT PEER-REVIEWED | Posted: 22 November 2022 doi:10.20944/preprints202211.0402.v1



22.20. For biomass-to-$H_2O$ ratio of 1:20, a peak of graphite of medium intensity (59.38%) was observed on the position 2θ: 26.47, and peaks characteristic of crystalline cellulose [20,77], of high intensity (79.0%) and (90.0%), on the positions 2θ: 15.53 and 2θ: 21.96, respectively. The results identified the occurrence of peaks of lower intensity of crystalline cellulose as the biomass-to-H2O ratio decreases, being in agreement to the results illustrated in Table 1.

*3.2. Process parameters, mass balances, and yields of reaction products*

***3.2.1 Influence of reaction time***

Table 2 summarizes the mass balances, process parameters and the yields of reaction products (hydro-char, aqueous, and gaseous phases) by hydrothermal processing of corn Stover at 250 °C, biomass/$H_2O$ ratio of 1:10, 60, 120, and 240 min, using a reactor of 18.927 L.

Table 2: Process parameters, mass balances, and yields of reaction products by hydrothermal carbonization of corn Stover at 250 °C, biomass/$H_2O$ proportion of 1:10, 60, 120 and 240 minutes, using a reactor of 18.927 L.

| Process parameters | 250 °C | | |
|---|---|---|---|
| | τ [min] | | |
| | 60 | 120 | 240 |
| Mass of Corn Straw [g] | 600.66 | 600.31 | 600.10 |
| Mass of $H_2O$ [g] | 6000.20 | 6002.70 | 6000.70 |
| Mechanical Stirrer Speed [rpm] | 90 | 90 | 90 |
| Initial Temperature [°C] | 30 | 30 | 30 |
| Heating Rate [°C/min] | 2 | 2 | 2 |
| Mass of Slurry [g] | 6482.40 | 6402.20 | 6425.10 |
| Volume of Gas [mL], T = 25 °C, P = 1 atm | 8405 | 12910 | 35225 |
| Mass of Gas [g] | 13.195 | 20.656 | 57.495 |
| Process Loss (I) [g] | 105.265 | 200.81 | 118.205 |
| Input Mass of Slurry (Pressing) [g] | 6474.70 | 6335.10 | 6417.80 |
| Process Loss (II) [g] | 7.70 | 7.10 | 7.30 |
| Mas of Liquid Phase [g] | 5034.80 | 5321 | 5288.90 |
| Mass of Moist Biochar [g] | 1262.18 | 898.42 | 976.64 |
| Process Loss (III) [g] | 177.72 | 115.68 | 152.26 |
| Mass of Dried Biochar [g] | 318.19 | 263.88 | 214.99 |
| Mass of $H_2O^{(V)}$ [g] | 943.99 | 634.54 | 761.65 |
| (Mas of Liquid Phase + Mass of $H_2O^{(V)}$) [g] | 5978.79 | 5955.54 | 6050.55 |
| Process Loss (I + II + III) [g] | 290.685 | 323.59 | 277.76 |
| Mass of $Liquid_{Reaction}$ [g] | 269.275 | 315.774 | 327.61 |
| Yield of Hydro-char [wt.%] | **52.97** | **43.96** | **35.82** |
| Yield of Gas [wt.%] | 2.19 | 3.44 | 9.58 |
| Yield of Liquid Phase [wt.%] | 44.84 | 52.60 | 54.59 |

Figure 11 shows the effect of reaction time on the yields of products (hydro-char, aqueous phase, and gas) by hydrothermal processing of corn Stover at 250 °C, biomass/$H_2O$ ratio of 1:10, 60, 120 and 240 min, using a reactor of 18.927 L. The yields of reaction products (hydro-char, aqueous phase, and gas) were regressed using exponential functions. The results show that applied exponential functions correlated well the experimental data for the solid, aqueous, and gaseous phases, with $R^2$ (R-Squared) between 0.994 and 0.999. The yield of hydro-char shows a smooth first-order exponential decay behavior, while that of the liquid and gaseous phases shows a smooth first-order exponential growth. The yield of hydro-char is according to similar data for the degradation of Brewer's Spent Grains [34], and maize silage [33].

Preprints (www.preprints.org) | NOT PEER-REVIEWED | Posted: 22 November 2022 doi:10.20944/preprints202211.0402.v1



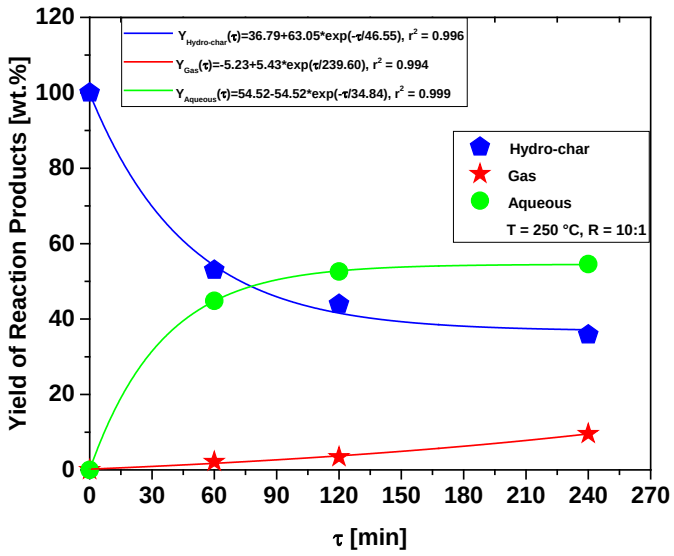


Figure 11. Yield of reaction products (hydro-char, aqueous phase, and gas) by hydrothermal processing of corn Stover at 250 °C, biomass-to-$H_2O$ ratio of 1:10, 60, 120, and 240 minutes, using a reactor of 18.927 L.

### *3.2.2 Influence of biomass-to-H2O ratio*

Table 3 summarizes the influence of biomass-to-$H_2O$ ratio on the mass balances, process parameters and the yields of reaction products (hydro-char, aqueous, and gaseous phases) by hydrothermal carbonization of corn Stover at 250 °C, 240 minutes, and biomass-to-$H_2O$ ratio of 1:10, 1:15, and 1:20, using a reactor of 18.927 L.

Table 3: Process parameters and material balances by hydrothermal carbonization of corn Stover at 250 °C, 240 minutes, biomass-to-$H_2O$ ratio of 1:10, 1:15, and 1:20, using a reactor of 18.927 L.

| Process parameters | 250 °C | | |
|---|---|---|---|
| | Biomass/$H_2O$ [-] | | |
| | 1:10 | 1:15 | 1:20 |
| Mass of corn Stover [g] | 600.10 | 600.11 | 600.28 |
| Mass of $H_2O$ [g] | 6000.70 | 9003.10 | 12007.00 |
| Mechanical Stirrer Speed [rpm] | 90 | 90 | 90 |
| Initial Temperature [°C] | 30 | 30 | 30 |
| Heating Rate [°C/min] | 2 | 2 | 2 |
| Process Time [min] | 240 | 240 | 240 |
| Mass of Slurry [g] | 6425.10 | 9488.90 | 11893.90 |
| Volume of Gas [mL], T = 25 °C, P = 1 atm | 35225 | 32536 | 30518 |
| Mass of Gas [g] | 57.495 | 52.546 | 48.534 |
| Process Loss (I) [g] | **118.205** | **61.764** | **664.846** |
| Input Mass of Slurry (Pressing) [g] | 6417.80 | 9476.40 | 11890.20 |
| Process Loss (II) [g] | **7.30** | **12.50** | **3.70** |
| Mas of Liquid Phase [g] | 5288.90 | 8544.30 | 10996.00 |
| Mass of Moist Biochar [g] | 976.64 | 851.06 | 782.45 |
| Process Loss (III) [g] | **152.26** | **81.04** | **111.75** |
| Mass of Dried Biochar [g] | 214.99 | 205.61 | 186.57 |
| Mass of $H_2O^{(V)}$ [g] | 761.65 | 645.45 | 595.88 |
| (Mas of Liquid Phase + Mass of $H_2O^{(V)}$) [g] | 6050.55 | 9189.75 | 11591.88 |
| Process Loss (I + II + III) [g] | **277.76** | **155.30** | **780.29** |
| Mass of $Liquid_{Reaction}$ [g] | 327.61 | 341.95 | 365.17 |
| Yield of Solids [wt.%] | 35.82 | 34.26 | 31.08 |
| Yield of Gas [wt.%] | 9.58 | 8.75 | 8.08 |
| Yield of Liquid Phase [wt.%] | 54.59 | 56.98 | 60.83 |

Preprints (www.preprints.org) | NOT PEER-REVIEWED | Posted: 22 November 2022 doi:10.20944/preprints202211.0402.v1



Figure 12 illustrates the influence of biomass-to-$H_2O$ ratio on the yield of reaction products by hydrothermal carbonization of corn Stover at 250 °C, 240 minutes, biomass-to-H2O ratio of 1:10, 1:15, and 1:20, using a pilot scale slurry stirred tank reactor of 18.927 L. By analyzing the experimental data for yield of reaction products (hydro-char, aqueous phase, and gas), depicted in Figure 12, one observes a linear behavior for all the data set, showing a light decrease on the yields of hydro-char and gas with increasing $H_2O$-to-biomass ratio, while that of aqueous phase increases. The decrease on the yields of hydro-char is probably due to the fact the hydrolysis is dominant reaction mechanism, but not the only one, as the $H_2O$-to-biomass ratio increases from 10 to 20 [15]. As the $H_2O$-to-biomass ratio increases, hydrolysis of lign-cellulosic material in biomass is enhanced [72-73], producing sugars (glucose, fructose, etc.), which are decomposed into volatile carboxylic acids, particularly acetic formic and acetic acids [31, 72-73]. On the other hand, as the monosaccharides (glucose, fructose, etc.) decomposes into low-chain carboxylic acids such as acetic acid [31, 72-73], dissociating within hot compressed $H_2O$ ($CH_3COOH + H_2O \rightarrow CH3COO^- + H^3O^+$), hydroxonium ions ($H^3O^+$) are formed due to dissociation of $CH_3COOH$ in $H_2O$, producing an acid aqueous media that decomposes hemicellulose and cellulose, improving the degradation of biomass, as shown in Table 3. An increase in the $H_2O$-to-biomass ratio enhances the biomass degradation, demonstrating that hydrolysis and isomerization steps were probably the dominant reaction mechanism, while the condensation, polymerization and nucleation steps were incomplete. This is according to the reaction mechanism proposed by Wang *et al.* [65], as an increase in the $H_2O$-to-biomass ratio produced a solid phase with low carbon content, *demonstrating that $H_2O$-to-biomass-to-$H_2O$ ratio of 1:20 was not enough to carbonize corn Stover, as shown in Figure 3.*

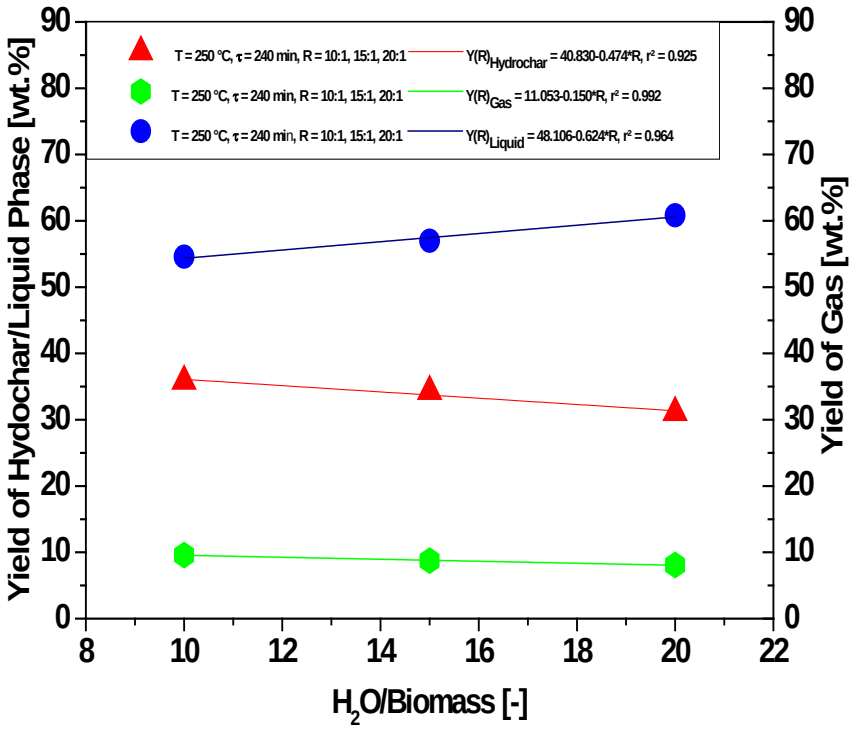


Figure 12. Yield of reaction products (hydro-char, aqueous phase, and gas) by hydrothermal processing of corn Stover at 250 °C, 240 minutes, and $H_2O$-to-biomass ratio of 10, 15, and 20, using a reactor of 18.927 L.

A smooth decrease on the yield of hydro-char with increasing $H_2O$-to-biomass ratio was also observed by Kang *et al.* [20], Arauzo *et al.* [34], Putra *et al.* [36], Putra *et al.* [40], Rather *et al.* [44], Rather *et al.* [46], Heilmann *et al.* [48], Putra *et al.* [52], Kambo *et al.* [57],

Preprints (www.preprints.org) | NOT PEER-REVIEWED | Posted: 22 November 2022 doi:10.20944/preprints202211.0402.v1



Sliz *et al.* [61], and Sabio *et al.* [62], showing the effect of $H_2O$-to-biomass ratio on the yield of hydro-char is according to similar studies reported in the literature [20,34,36,40,44,46,48,52,57,61-62].

### 3.2.3 *Degradation kinetics of corn Stover*

Figure 13 summarizes the experimental data for the degradation kinetics of corn Stover by hydrothermal processing at 250 °C, biomass-to-$H_2O$ ratio of 1:10, 60, 120 and 240 min, expressed as hydro-char formation. The kinetic data was correlated with a pseudo-first order exponential model described in section 2.7, and the experimental data compared to similar studies reported in the literature [33-34,36,40,44,60,75,78].

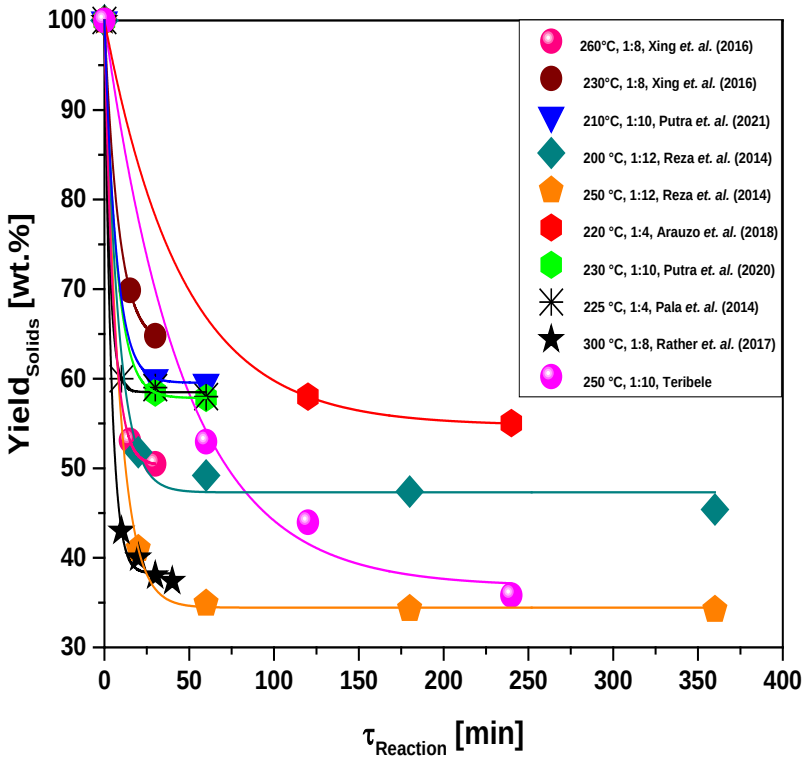


Figure 13. Kinetics of corn Stover degradation by hydrothermal processing of corn Stover at 250 °C, biomass/$H_2O$ ratio of 1:10, 60, 120, and 240 min, using a reactor of 18.927 L, compared with similar kinetic data reported in the literature [33-34,36,40,44,60,75,78].

Table 4: Regression of experimental kinetic data for the yield of hydro-char obtained by hydrothermal processing of corn Stover with hot compressed $H_2O$ at 250 °C, biomass-to-$H_2O$ ratio of 1:10, 240 minutes, using equation (16), compared with similar kinetic data reported in the literature [33-34,36,40,44,60,75,78].

| Kinetic Data [33-34,36,40,44,60,75,78] | *Regression of Experimental Kinetic Data* | | | | | |
|---|---|---|---|---|---|---|
| | *Process Parameters* | | | *Kinetic Parameters* | | |
| | T [°C] | Biomass/H2O [-] | τ [min] | A | K [$s^{-1}$] | $R^2$ |
| Xing *et al.* (2016) | 260 | 1:8 | 0, 15, 30 | 50.33 | 0.19231 | 1.000 |
| Xing *et al.* (2016) | 230 | 1:8 | 0, 15, 30 | 63.77 | 0.11880 | 1.000 |
| Putra *et al.* (2021) | 210 | 1:10 | 0, 30, 60 | 59.54 | 0.14536 | 1.000 |
| Reza *et al.* (2014) | 200 | 1:12 | 0, 20, 60, 180, 360 | 47.31 | 0.12266 | 1.000 |
| Reza *et al.* (2014) | 250 | 1:12 | 0, 20, 60, 180, 360 | 34.44 | 0.11501 | 1.000 |
| Arauzo *et al.* (2018) | 220 | 1:4 | 0, 120, 240 | 54.77 | 0.02199 | 1.000 |
| Putra *et al.* (2020) | 230 | 1:10 | 0, 30, 60 | 57.84 | 0.14070 | 1.000 |
| Pala *et al.* (2014) | 225 | 1:4 | 0, 10, 30, 60 | 58.50 | 0.33176 | 1.000 |
| Rather *et al.* (2017) | 300 | 1:8 | 0, 10, 20, 30, 40 | 38.26±0.71 | 0.2273-0.2835 | 0.999 |
| Teribele | 250 | 1:10 | 0, 60, 120, 240 | 36.79 | 0.02148 | 1.000 |

 doi:10.20944/preprints202211.0402.v1



The constant A, defined as $a/M_{Solids}(\tau)$], is included as a correction term, exhibiting a root-mean-square error ($r^2$) between 0.999 and 1.000, as shown in Table 4. In addition, by analyzing the experimental kinetic data illustrated in Figure 13, one observes the exponential decay behavior for all the data set, demonstrating that degradation kinetics of biomass with hot compressed $H_2O$, expressed as hydro-char formation, is well described by an exponential decay kinetics, as reported elsewhere [37-41].

### *3.2.4 Physicochemical analysis of Hydro-char*

Table 5 shows the elemental and physicochemical analysis of hydro-char by carbonization of corn Stover at 250 °C, biomass-to-$H_2O$ ratio of 1:10, reaction time of 60, 120, and 240 minutes, using a pilot scale stirred tank reactor of 5.0 gal. The elemental analysis illustrates, for constant biomass-to-$H_2O$ ratio, that carbon content increases with reaction time, while that of oxygen decreases, demonstrating that higher reaction times enhances the carbonization of corn Stover, as corroborate by the TG/DTG, MEV/EDX, and XRD analysis described in section 3.1

Table 5: Elemental characterization of hydro-char obtained by hydrothermal carbonization of corn Stover at 250 °C, biomass-to-$H_2O$ ratio of 1:10, reaction time of 60, 120, and 240 minutes, using a pilot scale stirred tank reactor of 5.0 gal.

| **Elemental Analysis/Physicochemical properties** | *Hydro-char* | | |
|---|---|---|---|
| | *250 °C* | | |
| | τ [min] | | |
| | **60** | **120** | **240** |
| **TS 60-105 °C [%MM]** | 98.65 | 97.26 | 97.75 |
| **OTS [%TS]** | 89.17 | 92.61 | 88.49* |
| **Ash [%TS]** | 9.48 | 4.65 | 9.26 |
| **N [%TS]** | 0.5629 | 0.9846 | 0.8611 |
| **C [%TS]** | 50.57 | 55.74 | 59.17 |
| **S [%TS]** | 0.1885 | 0.2224 | 0.2353 |
| **H [%TS]** | 6.571 | 6.97 | 5.719 |
| **O [%TS]** | 32.63 | 31.40 | 24.75 |

## 4. Conclusions

The principle of mass conservation, described in terms of a material balance, by hydrothermal processing of corn Stover with hot compressed $H_2O$, shows the yields of solid and gas phases decrease linearly with decreasing biomass-to-$H_2O$ ratio, while that of liquid phases increases linearly, maintaining the reaction time constant. In addition, the yield of solids decreases exponentially by decreasing the reaction time, while the yields of liquid and gas phases increase exponentially, for constant biomass-to-$H_2O$ ratio.

TG/DTG analysis of hydro-char shows that reaction time of 60 minutes was not enough to carbonize corn Stover, while an increase on the $H_2O$-to-biomass ratio worse the carbonization of corn Stover.

For constant biomass-to-$H_2O$ ratio, the SEM images show the main morphological structure of the corn Stover remains practically unchanged, while for constant reaction time, SEM images show that plant microstructure retains part of its original morphology, demonstrating that a decrease on biomass-to-$H_2O$ ratio worse the carbonization of corn Stover. For constant biomass-to-$H_2O$ ratio, the EDX analysis shows that the carbon content in hydro-char increases with reaction time, while for constant reaction time, the carbon content decreases with increasing biomass-to-$H_2O$ ratio. The kinetic of corn Stover degradation was correlated with a pseudo-first order exponential model, exhibiting a root-mean-square error ($r^2$) of 1.000, demonstrating that degradation kinetics of corn Stover with hot compressed $H_2O$, expressed as hydro-char formation, is well described by an exponential decay kinetics.

**Supplementary Materials:** The following materials are available. Figure S1: : SEM of hydro-char obtained after hydrothermal processing of corn Stover at 250 °C (Mag: 1000x), 60 minutes, and biomass-to-$H_2O$ ratio of 1:10, using a pilot scale stirred tank reactor of 5.0 gallon., Figure S2: SEM of

hydro-char obtained after hydrothermal processing of corn Stover at 250 °C (Mag: 5000x), 60 minutes, and biomass-to-$H_2O$ ratio of 1:10, using a pilot scale stirred tank reactor of 5.0 gallon., Figure S3: SEM of hydro-char obtained after hydrothermal processing of corn Stover at 250 °C (Mag: 1000x), 120 minutes, and biomass-to-$H_2O$ ratio of 1:10, using a pilot scale stirred tank reactor of 5.0 gallon., Figure S4: SEM of hydro-char obtained after hydrothermal processing of corn Stover at 250 °C (Mag: 5000x), 120 minutes, and biomass-to-$H_2O$ ratio of 1:10, using a pilot scale stirred tank reactor of 5.0 gallon., Figure S5: SEM of corn Stover after hydrothermal processing at 250 °C, 240 m, and biomass to-water ratio of 1:10, using a pilot scale stirred tank reactor of 5.0 gallon (Mag: 1000x)., Figure S6: SEM of hydro-char obtained after hydrothermal processing of corn Stover at 250 °C (Mag: 5000x), 240 m, and biomass to-water ratio of 1:10, using a pilot scale stirred tank reactor of 5.0 gallon., Figure S7: SEM of hydro-char obtained after hydrothermal processing of corn Stover at 250 °C (Mag: 20000x), 240 minutes, and biomass-to-$H_2O$ ratio of 1:10, using a pilot scale stirred tank reactor of 5.0 gallon., Figure S8: SEM of hydro-char obtained after hydrothermal processing of corn Stover at 250 °C (Mag: 1000x), 240 minutes, and biomass-to-$H_2O$ ratio of 1:15, using a pilot scale stirred tank reactor of 5.0 gallon., Figure S9: SEM of hydro-char obtained after hydrothermal processing of corn Stover at 250 °C (Mag: 2500x), 240 minutes, and biomass-to-$H_2O$ ratio of 1:15, using a pilot scale stirred tank reactor of 5.0 gallon., Figure S10: SEM of hydro-char obtained after hydrothermal processing of corn Stover at 250 °C (Mag: 5000x), 240 minutes, and biomass-to-$H_2O$ ratio of 1:15, using a pilot scale stirred tank reactor of 5.0 gallon., Figure S11: SEM of hydro-char obtained after hydrothermal processing of corn Stover at 250 °C (Mag: 1000x), 240 minutes, and biomass-to-water ratio of 1:20, using a pilot scale stirred tank reactor of 5.0 gallon., Figure S12: SEM of hydro-char obtained after hydrothermal processing of corn Stover at 250 °C (Mag: 2500x), 240 minutes, and biomass-to-water ratio of 1:20, using a pilot scale stirred tank reactor of 5.0 gallon., Figure S13: SEM of hydro-char obtained after hydrothermal processing of corn Stover at 250 °C (Mag: 5000x), 240 minutes, and biomass-to-water ratio of 1:20, using a pilot scale stirred tank reactor of 5.0 gallon.

**Author Contributions:** The individual contributions of all the co-authors are provided as follows: T.T. contributed with formal analysis and writing original draft preparation, M.E.G.C. contributed with formal analysis and methodology, C.d.M.S.d.S. contributed with formal analysis and methodology, L.M.P. contributed with formal analysis and chemical analysis, L.P.B. contributed with formal analysis and methodology, F.P.d.C.A. contributed with formal analysis and methodology, I.W.d.S.B. contributed with chemical analysis, C.J.N.F. contributed with chemical analysis, S.J.B. contributed with formal analysis, M.C.S. contributed with formal analysis and methodology, T.H. contributed with resources and infrastructure, M.S. contributed with investigation and chemical analysis, D.A.R.d.C. with co-supervision and with formal analysis, and N.T.M. contributed with supervision, conceptualization, and data curation. All authors have read and agreed to the published version of the manuscript.

**Funding**: This research received no external funding.

**Institutional Review Board Statement**: Not applicable.

**Informed Consent Statement**: Not applicable.

**Acknowledgments:** I would like to acknowledge and dedicate this research in memory to Hélio da Silva Almeida, he used to work at the Faculty of Sanitary and Environmental Engineering/UFPa, and passed away on 13 March 2021. His contagious joy, dedication, intelligence, honesty, seriousness, and kindness will always be remembered in our hearts.

**Conflicts of Interest:** The authors declare no conflict of interest.

## References

1. Maria Cristina Dias Paes, Flavia França Teixeira, Ileane Samara Martins. Composição Química da Palha de Milho com Qualidade para Artesanato. https://www.alice.cnptia.embrapa.br/alice/bitstream/doc/491365/1/Composicaoquimica.pdf
2. Shishir P. S. Chundawat, Balan Venkatesh, Bruce E. Dale. Effect of Particle Size Based Separation of Milled Corn Stover on AFEX Pretreatment and Enzymatic Digestibility. Biotechnol. Bioeng. 2007; 96: 219–231
3. World Corn Production by Country. https://www.atlasbig.com/en-us/world-corn-production-map
4. Salazar, R. F. S., Silva, G. L. P., Silva, M. L. C. P. Estudo da Composição da Palha de Milho Para Posterior Utilização Como Suporte na Preparação de Compósitos. VI Congresso Brasileiro de Engenharia Química em Iniciação Científica, 2005, UNICAMP.https://docplayer.com.br/53288584-Estudo-da-composicao-da-palha-de-milho-para-posterior-utilizacao-como-suporte-na-preparacao-de-compositos.html

5. N. T. Machado, D. A. R. de Castro, L. S. Queiroz, M. C. Santos, C. E. F. da Costa. Production and Characterization of Energy Materials with Adsorbent Properties by Hydrothermal Processing of Corn Stover with Subcritical $H_2O$. Journal of Applied Solution Chemistry and Modeling, Volume 5, N° 3, 117-130
6. N.T. Machado, D.A.R. de Castro, M.C. Santos, M.E. Araújo, U. Lüder, L. Herklotz, M. Werner, J. Mumme, T. Hoffmann. Process analysis of hydrothermal carbonization of corn Stover with subcritical $H_2O$. The Journal of Supercritical Fluids 136 (2018) 110–122
7. Maria Elizabeth Gemaque Costa, Fernanda Paula da Costa Assunção, Tiago Teribele, Lia Martins Pereira, Douglas Alberto Rocha de Castro, Marcelo Costa Santo, Carlos Emerson Ferreira da Costa, Maja Shultze, Thomas Hofmann, Nélio Teixeira Machado. Characterization of Bio-Adsorbents Produced by Hydrothermal Carbonization of Corn Stover: Application on the Adsorption of Acetic Acid from Aqueous Solutions. Energies 2021, 14, 8154. https://doi.org/10.3390/en14238154
8. Funke, A., Ziegler, F. Hydrothermal carbonization of biomass: a summary and discussion of chemical mechanisms for process engineering. Biofuels, Bioprod. Biorefin. 4 (2010), 160–177
9. Roland Becker, Ute Dorgerloh, Ellen Paulke, Jan Mumme, Irene Nehls. Hydrothermal Carbonization of Biomass: Major Organic Components of the Aqueous Phase. *Chem. Eng. Technol.* 2014, *37*, N°. 3, 511–518
10. J. A. Libra, K. S. Ro, C. Kammann, A. Funke, N. D. Berge, Y. Neubauer, M. M. Titirici, C. Fühner, O. Bens, J. Kern, K. H. Emmerich. Hydrothermal carbonization of biomass residuals: a comparative review of the chemistry, processes and applications of wet and dry pyrolysis. Biofuels 2011, 2 (1), 89–124
11. Ivo Oliveira, Dennis Blöhse, Hans-Günter Ramke. Hydrothermal carbonization of agricultural residues. Bioresour. Technol. 142 (2013) 138–146
12. M. Toufiq Reza, Benjamin Wirth, Ulf Lüder, Maja Werner. Behavior of selected hydrolyzed and dehydrated products during hydrothermal carbonization of biomass. Bioresource Technology, Volume 169, October 2014, 352–361
13. Zhengang Liu, Rajasekhar Balasubramanian. Upgrading of waste biomass by hydrothermal carbonization (HTC) and low temperature pyrolysis (LTP): A comparative evaluation. Applied Energy 114 (2014) 857–864
14. S. Kent Hoekman, Amber Broch, Curtis Robbins, Barbara Zielinska, Larry Felix. Hydrothermal carbonization (HTC) of selected woody and herbaceous biomass feedstocks. Biomass Convers. Bioref. 3 (2013) 113–126
15. Conceição de Maria Sales da Silva, Douglas Alberto Rocha de Castro, Marcelo Costa Santos, Hélio da Silva Almeida, Maja Schultze, Ulf Lüder, Thomas Hoffmann, Nélio Teixeira Machado. Process Analysis of Main Organic Compounds Dissolved in Aqueous Phase by Hydrothermal Processing of Açaí (Euterpe oleraceae, Mart.) Seeds: Influence of Process Temperature, Biomass-to-Water Ratio, and Production Scales. Energies 2021, 14, 5608. https://doi.org/10.3390/en14185608
16. A.B. Fuertes, M. Camps Arbestain, M. Sevilla, J.A. Maciá-Agulló, S. Fiol, R. López, R.J. Smernik, W.P. Aitkenhead, F. Arce, F. Macias. Chemical and structural properties of carbonaceous products obtained by pyrolysis and hydrothermal carbonization of corn stover. Aust. J. Soil Res. 48 (7) (2010) 618–626
17. Ling-Ping Xiao, Zheng-Jun Shi, Feng Xu, Run-Cang Sun. Hydrothermal carbonization of lignocellulosic biomass. Bioresour. Technol. 18 (2012) 619–623
18. Mohammad Toufiqur Reza. Upgrading Biomass by Hydrothermal and Chemical Conditioning. PhD Thesis, University of Nevada, Reno, May, 2013. https://www.researchgate.net/publication/245455351_Upgrading_Biomass_by_Hydrotherma and_Chemical_Conditioning
19. M. Toufiq Reza, Joan G. Lynam, M. Helal Uddin, Charles J. Coronella. Hydrothermal carbonization: fate of inorganics. Biomass Bioenergy 49 (2013) 86–94
20. Kang, K.; Sonil, N.; Guotao, S.; Ling, Q.; Yongqing, G.; Tianle, Z.; Mingqiang, Z.; Runcang, S. Microwave assisted hydrothermal carbonization of corn stalk for solid biofuel production: Optimization of process parameters and characterization of hydrochar. Energy 2019, 186, 115–125, doi:10.1016/j.energy.
21. Ibrahim Shaba Mohammed, Risu NA, Keisuke Kushima, Naoto Shimizu. Investigating the Effect of Processing Parameters on the Products of Hydrothermal Carbonization of Corn Stover. Susteinability 2020, 12, 5100, doi: 10.3390/su12125100
22. Sandeep Kumar, Urvi Kothari, Lingzhao Kong, Y.Y. Lee, Ram B. Gupta. Hydrothermal pretreatment of switchgrass and corn stover for production of ethanol and carbon microspheres. Biomass and Bioenergy 35 (2011) 956-968
23. Nathan Mosier, Richard Hendrickson, Nancy Ho, Miroslav Sedlak, Michael R. Ladisch. Optimization of pH controlled liquid hot water pretreatment of corn stover. Bioresource Technology 96 (2005) 1986–1993
24. Ying Zhang, Qun Jiang, Weiling Xie, Yifan Wang, Jiaming Kang. Effects of temperature, time and acidity of hydrothermal carbonization on the hydrochar properties and nitrogen recovery from corn stover. Biomass and Bioenergy 122 (2019) 175–182
25. Md Tahmid Islam, Nepu Saha, Sergio Hernandez, Jordan Klinger and M. Toufiq Reza. Integration of Air Classification and Hydrothermal Carbonization to Enhance Energy Recovery of Corn Stover. Energies 2021, 14, 1397. https://doi.org/10.3390/en14051397
26. Ren Tu, Yan Sun, Yujian Wu, Xudong Fan, Jiamin Wang, Shuchao Cheng, Zhiwen Jia, Enchen Jiang and Xiwei Xu. Improvement of corn stover fuel properties via hydrothermal carbonization combined with surfactant. Biotechnol Biofuels (2019) 12:249 https://doi.org/10.1186/s13068-019-1581-x
27. Feng Shen,Yu Wang, Luyang Li, Keqiang Zhang, Richard L. Smith, Xinhua Q. Porous carbonaceous materials from hydrothermal carbonization and KOH activation of corn stover for highly efficient $CO_2$ capture. Chemical Engineering Communications 205 (2018), Issue 4, 423-431

28. Li, L.; Flora, J.R.; Caicedo, J.M.; Berge, N.D. Investigating the role of feedstock properties and process conditions on products formed during the hydrothermal carbonization of organics using regression techniques. Bioresour. Technol. 2015, 187, 263–274
29. Hoekman, S.K.; Broch, A.; Robbins, C. Hydrothermal Carbonization (HTC) of Lignocellulosic Biomass. Energy Fuels 2011, 25, 1802–1810
30. Becker, R.; Dorgerloh, U.; Helmis, M.; Mumme, J.; Diakité, M.; Nehls, I. Hydrothermally carbonized plant materials: Patterns of volatile organic compounds detected by gas chromatography. Bioresour. Technol. 2013, 130, 621–628
31. Poerschmann, J.; Weiner, B.; Koehler, R.; Kopinke, F.D. Hydrothermal Carbonization of Glucose, Fructose, and XyloseIdentification of Organic Products with Medium Molecular Masses. ACS Sustainable Chem. Eng. 2017, 5, 6420–6428
32. Agnieszka Urbanowska, Małgorzata Kabsch-Korbutowicz, Mateusz Wnukowski, Przemysław Seruga, Marcin Baranowski, Halina Pawlak-Kruczek, Monika Serafin-Tkaczuk, Krystian Krochmalny and Lukasz Niedzwiecki. Treatment of Liquid By-Products of Hydrothermal Carbonization (HTC) of Agricultural Digestate Using Membrane Separation. Energies 2020, 13, 262; doi:10.3390/en13010262
33. M. Toufiq Reza, Wolfgang Becker, Kerstin Sachsenheimer, Jan Mumme. Hydrothermal carbonization (HTC): Near infrared spectroscopy and partial least-squares regression for determination of selective components in HTC solid and liquid products derived from maize silage. Bioresource Technology 161 (2014) 91–101
34. Pablo J. Arauzo, Maciej P. Olszewski and Andrea Kruse. Hydrothermal Carbonization Brewer's Spent Grains with the Focus on Improving the Degradation of the Feedstock. Energies 2018, 11, 3226; doi:10.3390/en11113226
35. P.J. Arauzo, L. Du, M.P. Olszewski, M.F. Meza Zavala, M.J. Alhnidi, A. Kruse. Effect of protein during hydrothermal carbonization of brewer's spent grain. Bioresource Technology 293 (2019) 122117
36. Herlian Eriska Putra, Enri Damanhuri, Kania Dewi, Ari Darmawan Pasek. Production of Coal-Like Solid Fuel from Albizia Chinensis Sawdust via Wet Torrefaction Process. Journal of Ecological Engineering 2020, 21(6), 183-190
37. M. Toufiq Reza, Wei Yan, M. Helal Uddin, Joan G. Lynam, S. Kent Hoekman, Charles J. Coronella, Victor R. Vásquez. Reaction kinetics of hydrothermal carbonization of loblolly pine. Bioresource Technology 139 (2013) 161–169
38. E. Danso-Boateng, R.G. Holdich, G. Shama, A.D. Wheatley, M. Sohail, S.J. Martin. Kinetics of faecal biomass hydrothermal carbonisation for hydrochar production. Applied Energy 111 (2013) 351–357
39. A. Alvarez-Murillo, E. Sabio, B. Ledesma, S. Roman, C.M. Gonzalez-García. Generation of biofuel from hydrothermal carbonization of cellulose. Kinetics modelling. Energy 94 (2016) 600-608
40. Herlian Eriska Putra, Djaenudin, Enri Damanhuri, Kania Dewi, Ari Darmawan Pasek. Hydrothermal Carbonization Kinetics of Lignocellulosic Municipal Solid Waste. Journal of Ecological Engineering 2021, 22(3), 188–198
41. Fengjun Yin, Hongzhen Chen, Guihua Xu, Guangwei Wang, Yuanjian Xu. A detailed kinetic model for the hydrothermal decomposition process of sewage sludge. Bioresource Technology 198 (2015) 351–357
42. Shuqing Guo, Xiangyuan Dong, Tingting Wu, Caixia Zhu. Influence of reaction conditions and feedstock on hydrochar properties. Energy Conversion and Management 123 (2016) 95–103
43. Ying Gao, Xianhua Wang, Jun Wang, Xiangpeng Li, Jianjun Cheng, Haiping Yang, Hanping Chen. Effect of residence time on chemical and structural properties of hydro-char obtained by hydrothermal carbonization of water hyacinth. Energy 58 (2013) 376-383
44. Mushtaq Ahmad Rather, N.S. Khan, Rajat Gupta. Hydrothermal carbonization of macrophyte Potamogeton lucens for solid biofuel: Production of solid biofuel from macrophyte Potamogeton lucens. Engineering Science and Technology, an International Journal 20 (2017) 168–174
45. Herlian Eriska Putra, Kania Dewi, Enri Damanhuri, Ari Darmawan Pasek. Conversion of organic fraction of municipal solid waste into solid fuel via hydrothermal carbonization. International Journal of Engineering & Technology, 7 (4) (2018) 4030-4034
46. M. A. Rather, N. S. Khan, R. Gupta. Catalytic hydrothermal carbonization of invasive macrophyte Hornwort (Ceratophyllum demersum) for production of hydrochar: a potential biofuel. Int. J. Environ. Sci. Technol. (2017) 14:1243–1252
47. Zebin Cao, Dennis Jung, Maciej P. Olszewski, Pablo J. Arauzo, Andrea Kruse. Hydro-thermal carbonization of biogas digestate: Effect of digestate origin and process conditions. Waste Management 100 (2019) 138–150
48. Steven M. Heilmann, Lindsey R. Jader, Michael J. Sadowsky, Frederick J. Schendel, Marc G. von Keitz, Kenneth J. Valentas. Hydrothermal carbonization of distiller's grains. Biomass and bioenergy 35 (2011) 2526-2533
49. Mikko Mäkelä, Verónica Benavente, Andrés Fullana. Hydrothermal carbonization of lignocellulosic biomass: Effect of process conditions on hydrochar properties. Applied Energy 155 (2015) 576–584
50. Ke Wu, Xin Zhang, Qiaoxia Yuan. Effects of process parameters on the distribution characteristics of inorganic nutrients from hydrothermal carbonization of cattle manure. Journal of Environmental Management 209 (2018) 328-335
51. Asli Toptas Tag, Gozde Duman, Jale Yanik. Influences of feedstock type and process variables on hydrochar properties. Bioresource Technology 250 (2018) 337–344
52. Herlian Eriska Putra, Enri Damanhuri, Kania Dewi and Ari Darmawan Pasek. Hydrothermal carbonization of biomass waste under low temperature condition. MATEC Web of Conferences 154, 01025 (2018), https://doi.org/10.1051/matecconf/201815401025
53. Xiaowei Lu, Perry J. Pellechia, Joseph R.V. Flora, Nicole D. Berge. Influence of reaction time and temperature on product formation and characteristics associated with the hydrothermal carbonization of cellulose. Bioresource Technology 138 (2013) 180–190

54. Chao He, Apostolos Giannis, Jing-Yuan Wang. Conversion of sewage sludge to clean solid fuel using hydrothermal carbonization: Hydrochar fuel characteristics and combustion behavior. Applied Energy 111 (2013) 257–266
55. Lei Zhang, Shanshan Liu, Baobin Wang, Qiang Wang, Guihua Yang, Jiachuan Chen. Effect of Residence Time on Hydrothermal Carbonization of Corn Cob Residual. BioResouces 10(3), 3979-3986
56. Verónica Benavente, Emilio Calabuig, Andres Fullana. Upgrading of moist agro-industrial wastes by hydrothermal carbonization. Journal of Analytical and Applied Pyrolysis 113 (2015) 89–98
57. Harpreet Singh Kambo, Animesh Dutta. Comparative evaluation of torrefaction and hydrothermal carbonization of lignocellulosic biomass for the production of solid biofuel. Energy Conversion and Management 105 (2015) 746–755
58. Xiaowei Lu, Nicole D. Berge. Influence of feedstock chemical composition on product formation and characteristics derived from the hydrothermal carbonization of mixed feedstocks. Bioresource Technology 166 (2014) 120–131
59. Xiaowei Lu, Joseph R.V. Flora, Nicole D. Berge. Influence of process water quality on hydrothermal carbonization of celulose. Bioresource Technology 154 (2014) 229–239
60. Mehmet Pala, Ismail Cem Kantarli, Hasan Baha Buyukisik, Jale Yanik. Hydrothermal carbonization and torrefaction of grape pomace: A comparative evaluation. Bioresource Technology 161 (2014) 255–262
61. Maciej Sliz, Małgorzata Wilk. A comprehensive investigation of hydrothermal carbonization: Energy potential of hydrochar derived from Virginia mallow. Renewable Energy 156 (2020) 942-950
62. E. Sabio, A. Álvarez-Murillo, S. Román, B. Ledesma. Conversion of tomato-peel waste into solid fuel by hydrothermal carbonization: Influence of the processing variables. Waste Management 47 (2016) 122–132
63. Xiuzheng Zhuang, Hao Zhan, Yanpei Song, Chao He, Yanqin Huang, Xiuli Yin, Chuangzhi Wu. Insights into the evolution of chemical structures in lignocellulose and nonlignocellulose biowastes during hydrothermal carbonization (HTC). Fuel 236 (2019) 960–974
64. Shuqing Guo, Xiangyuan Dong, Tingting Wu, Fengjuan Shi, Caixia Zhu. Characteristic evolution of hydrochar from hydrothermal carbonization of corn stalk. Journal of Analytical and Applied Pyrolysis 116 (2015) 1–9
65. Tengfei Wang, Yunbo Zhai, Yun Zhu, Caiting Li, Guangming Zeng. A review of the hydrothermal carbonization of biomass waste for hydrochar formation: Process conditions, fundamentals, and physicochemical properties. Renewable and Sustainable Energy Reviews 90 (2018) 223–247
66. Akshay Jain, Rajasekhar Balasubramanian, M.P. Srinivasan. Hydrothermal conversion of biomass waste to activated carbon with high porosity: A review. Chemical Engineering Journal 283 (2016) 789–805
67. Silvia Román, Judy Libra, Nicole Berge, Eduardo Sabio, Kyoung Ro, Liang Li, Beatriz Ledesma, Andrés Álvarez and Sunyoung Bae. Hydrothermal Carbonization: Modeling, Final Properties Design and Applications: A Review. Energies 2018, 11, 216; doi:10.3390/en11010216
68. Manfredi Picciotto Maniscalco, Maurizio Volpe and Antonio Messineo. Hydrothermal Carbonization as a Valuable Tool for Energy and Environmental Applications: A Review. Energies 2020, 13, 4098; doi:10.3390/en13164098
69. Sabzoi Nizamuddin, N.M. Mubarak, Manoj Tiripathi, N.S. Jayakumar, J.N. Sahu, P. Ganesan. Chemical, dielectric and structural characterization of optimized hydrochar produced from hydrothermal carbonization of palm shell. Fuel 163 (2016) 88–97
70. J. A. Libra, K. S. Ro, C. Kammann, A. Funke, N. D. Berge, Y. Neubauer, M. M. Titirici, C. Fühner, O. Bens, J. Kern, K. H. Emmerich. Hydrothermal carbonization of biomass residuals: a comparative review of the chemistry, processes and applications of wet and dry pyrolysis. Biofuels 2011, 2 (1), 89–124
71. Sittisun, P.; Tippayawong, N.; Wattanasiriwech, D. Thermal Degradation characteristics and kinetics of oxy combustion of corn residues. Adv. Mater. Sci. Eng. 2015, 2015, 1–8
72. Román, S.; Nabais, J.M.V.; Laginhas, C.; Ledesma, B.; González, J.F. Hydrothermal carbonization as an effective way of densifying the energy content of biomass. Fuel Process. Technol. 2012, 103, 78–83
73. Sermyagina, E.; Saari, J.; Kaikko, J.; Vakkilainen, E. Hydrothermal carbonization of coniferous biomass: Effect of process parameters on mass and energy yields. J. Anal. Appl. Pyrolysis 2015, 113, 551–556
74. Sevilla, M.; Fuertes, A.B. The production of carbon materials by hydrothermal carbonization of cellulose. Carbon 2009, 47, 2281–2289
75. Xianjun Xing, Fangyu Fan, Suwei Shi, Yongqiang Xing, Yongling Li, Xuefei Zhang, Jing Yang. Fuel Properties and Combustion Kinetics of Hydrochar Prepared by Hydrothermal Carbonization of Corn Straw. *BioResources 11(4), 9190-9204*
76. Hoskinson, R.L.; Karlen, D.L.; Birrell, S.J.; Radtke, C.W.; Wilhelm, W.W. Engineering, nutrient removal, and feedstock conversion evaluations of four corn stover harvest scenarios. Biomass Bioenergy 2007, 31, 126–136
77. Regmi, P.; Moscoso, J.L.G.; Kumar, S.; Cao, X.; Mao, J.; Schafran, G. Removal of copper and cadmium from aqueous solution using switchgrass biochar produced via hydrothermal carbonization process. J. Environ. Manag. 2012, 109, 61–69
78. H E Putra, E Damanhuri, K Dewi, A D Pasek. Hydrothermal treatment of municipal solid waste into coallike fuel. IOP Conf. Series: Earth and Environmental Science 483 (2020) 012021 doi:10.1088/1755-1315/483/1/012021